Biogeosciences, 12, 653–679, 2015
www.biogeosciences.net/12/653/2015/
doi:10.5194/bg-12-653-2015


Biogeosciences Open Access

# Recent trends and drivers of regional sources and sinks of carbon dioxide

**S. Sitch[1], P. Friedlingstein[1], N. Gruber[2], S. D. Jones[3], G. Murray-Tortarolo[1], A. Ahlström[4], S. C. Doney[5], H. Graven[6], C. Heinze[7,8,9], C. Huntingford[10], S. Levis[11], P. E. Levy[12], M. Lomas[13], B. Poulter[14], N. Viovy[15], S. Zaehle[16], N. Zeng[17], A. Arneth[18], G. Bonan[11], L. Bopp[15], J. G. Canadell[19], F. Chevallier[15], P. Ciais[15], R. Ellis[10], M. Gloor[20], P. Peylin[15], S. L. Piao[21], C. Le Quéré[3], B. Smith[4], Z. Zhu[22,23], and R. Myneni[24]**

[1]University of Exeter, Exeter EX4 4QF, UK
[2]Institute of Biogeochemistry and Pollutant Dynamics, ETH Zurich, Zurich, Switzerland
[3]Tyndall Centre for Climate Change Research, University of East Anglia, Norwich NR4 7TJ, UK
[4]Lund University, Department of Physical Geography and Ecosystem Science, Sölvegatan 12, 223 62 Lund, Sweden
[5]Marine Chemistry and Geochemistry Department, Woods Hole Oceanographic Institution, 266 Woods Hole Road, Woods Hole, MA 02543, USA
[6]Department of Physics and Grantham Institute for Climate Change, Imperial College London, London SW7 2AZ, UK
[7]Geophysical Institute, University of Bergen, Bergen, Norway
[8]Bjerknes Centre for Climate Research, Bergen, Norway
[9]Uni Climate, Uni Research AS, Bergen, Norway
[10]Centre for Ecology and Hydrology, Benson Lane, Wallingford OX10 8BB, UK
[11]National Center for Atmospheric Research, Boulder, Colorado, USA
[12]Centre for Ecology and Hydrology, Bush Estate, Penicuik, Midlothian EH26 0QB, UK
[13]Department of Animal & Plant Sciences, University of Sheffield, Sheffield S10 2TN, UK
[14]Institute on Ecosystems and Department of Ecology, Montana State University, Bozeman, MT 59717, USA
[15]Laboratoire des Sciences du Climat et de l'Environnement, CEA CNRS UVSQ, 91191 Gif-sur-Yvette, France
[16]Biogeochemical Integration Department, Max Planck Institute for Biogeochemistry, P.O. Box 10 01 64, 07701 Jena, Germany
[17]Department of Atmospheric and Oceanic Science, University of Maryland, College Park, MD 20740, USA
[18]Karlsruhe Institute of Technology, Garmisch-Partenkirchen, Germany
[19]Global Carbon Project, CSIRO Oceans and Atmosphere Flagship, Canberra, Australia
[20]University of Leeds, School of Geography, Woodhouse Lane, Leeds LS9 2JT, UK
[21]College of Urban and Environmental Sciences, Peking University, Beijing 100871, China
[22]State Key Laboratory of Remote Sensing Science, Institute of Remote Sensing and Digital Earth, Chinese Academy of Sciences, Beijing 100101, China
[23]Center for Applications of Spatial Information Technologies in Public Health, Beijing 100101, China
[24]Department of Geography and Environment, Boston University, 675 Commonwealth Avenue, Boston, MA 02215, USA

*Correspondence to:* S. Sitch (s.a.sitch@exeter.ac.uk)

Received: 21 November 2013 – Published in Biogeosciences Discuss.: 23 December 2013
Revised: 30 November 2014 – Accepted: 19 December 2014 – Published: 2 February 2015

**Published by Copernicus Publications on behalf of the European Geosciences Union.**

**Abstract.** The land and ocean absorb on average just over half of the anthropogenic emissions of carbon dioxide ($CO_2$) every year. These $CO_2$ "sinks" are modulated by climate change and variability. Here we use a suite of nine dynamic global vegetation models (DGVMs) and four ocean biogeochemical general circulation models (OBGCMs) to estimate trends driven by global and regional climate and atmospheric $CO_2$ in land and oceanic $CO_2$ exchanges with the atmosphere over the period 1990–2009, to attribute these trends to underlying processes in the models, and to quantify the uncertainty and level of inter-model agreement. The models were forced with reconstructed climate fields and observed global atmospheric $CO_2$; land use and land cover changes are not included for the DGVMs. Over the period 1990–2009, the DGVMs simulate a mean global land carbon sink of $-2.4 \pm 0.7\,\mathrm{Pg\,C\,yr^{-1}}$ with a small significant trend of $-0.06 \pm 0.03\,\mathrm{Pg\,C\,yr^{-2}}$ (increasing sink). Over the more limited period 1990–2004, the ocean models simulate a mean ocean sink of $-2.2 \pm 0.2\,\mathrm{Pg\,C\,yr^{-1}}$ with a trend in the net C uptake that is indistinguishable from zero ($-0.01 \pm 0.02\,\mathrm{Pg\,C\,yr^{-2}}$). The two ocean models that extended the simulations until 2009 suggest a slightly stronger, but still small, trend of $-0.02 \pm 0.01\,\mathrm{Pg\,C\,yr^{-2}}$. Trends from land and ocean models compare favourably to the land greenness trends from remote sensing, atmospheric inversion results, and the residual land sink required to close the global carbon budget. Trends in the land sink are driven by increasing net primary production (NPP), whose statistically significant trend of $0.22 \pm 0.08\,\mathrm{Pg\,C\,yr^{-2}}$ exceeds a significant trend in heterotrophic respiration of $0.16 \pm 0.05\,\mathrm{Pg\,C\,yr^{-2}}$ – primarily as a consequence of widespread $CO_2$ fertilisation of plant production. Most of the land-based trend in simulated net carbon uptake originates from natural ecosystems in the tropics ($-0.04 \pm 0.01\,\mathrm{Pg\,C\,yr^{-2}}$), with almost no trend over the northern land region, where recent warming and reduced rainfall offsets the positive impact of elevated atmospheric $CO_2$ and changes in growing season length on carbon storage. The small uptake trend in the ocean models emerges because climate variability and change, and in particular increasing sea surface temperatures, tend to counteract the trend in ocean uptake driven by the increase in atmospheric $CO_2$. Large uncertainty remains in the magnitude and sign of modelled carbon trends in several regions, as well as regarding the influence of land use and land cover changes on regional trends.

## 1 Introduction

Soon after the first high-precision measurements of atmospheric $CO_2$ started in the late 1950s, it became clear that the global-mean $CO_2$ growth rate is substantially lower than expected if all anthropogenic $CO_2$ emissions remained in the atmosphere (e.g. Keeling et al., 1976). The search for this "missing" carbon and the identification of the processes driving carbon sinks has been one of the dominating questions for carbon cycle research in the past decades (e.g. Tans et al., 1990; Sarmiento and Gruber, 2002; and others). While much progress has been achieved (e.g. Prentice et al., 2001; Sabine et al., 2004; Denman et al., 2007; Le Quéré et al., 2009), and estimates have converged considerably (Sweeney et al., 2007; Khatiwala et al., 2013; Wanninkhof et al., 2013), the spatial attribution of recent sink rates for the ocean and land, and particularly their changes through time, remain uncertain. To balance the global carbon budget, the combined sinks by land and ocean must have increased over recent decades (Keeling et al., 1995; Canadell et al., 2007; Raupach et al., 2008; Sarmiento et al., 2010; Gloor et al., 2010; Ballantyne et al., 2012). Sarmiento et al. (2010) showed that some of the increasing sinks are driven by the ocean, but also identified an even more substantial increase in the net uptake by the land biosphere between the 1980s and the 1990s. This increase in the global land and ocean sink has been sustained to date (Ballantyne et al., 2012).

There are several studies on the trends in carbon exchanges at the regional level based on atmospheric $CO_2$ observations (top-down approach) (Angert et al., 2005; Buermann et al., 2007; Chevallier et al., 2010; Sarmiento et al., 2010) and changes in high-latitude greenness on land (Nemani et al., 2003; Myneni et al., 1997) and changes in sea surface temperature in the ocean (Park et al., 2010). Atmospheric $CO_2$-based top-down approaches provide large-scale constraints on the land and ocean surface processes, but they cannot unambiguously identify the underlying processes or the regions driving these changes. Bottom-up studies using dynamic global vegetation models (DGVMs) or ocean biogeochemical general circulation models (OBGCMs) mechanistically represent many of the key land (Prentice et al., 2007) and ocean processes (Le Quéré et al., 2005), and offer the opportunity to investigate how changes in the structure and functioning of land ecosystems and the ocean in response to changing environmental conditions affect biogeochemical cycles. Therefore DGVMs and OBGCMs potentially allow for a more comprehensive analysis of surface carbon trends and provide insight into possible mechanisms behind regional trends in the carbon cycle.

There is a growing literature on regional carbon budgets for different parts of the world (Ciais et al., 1995; Phillips et al., 1998; Fan et al., 1998; Pacala et al., 2001; Janssens et al., 2003; Stephens et al., 2007; Piao et al., 2009; Lewis et al., 2009a; Ciais et al., 2010; Pan et al., 2011; Tjiputra et al., 2010; Roy et al., 2011; Schuster et al., 2013; Lenton et al., 2013), using bottom-up (inventory, carbon cycle models) and top-down methodologies, although they typically cover different time intervals. To date, no globally consistent attribution has been attempted for regional sources and sinks of atmospheric $CO_2$. This paper attempts to fill this gap by combining top-down and bottom-up approaches discussed in the regional syntheses of the REgional

Carbon Cycle Assessment and Processes project (RECCAP; Canadell et al., 2013) and by using factorial simulations to elucidate the processes that drive trends in the sources and sinks of atmospheric $CO_2$.

This study has two major aims. The first of these is to estimate the regional trends in the carbon exchange over the period 1990–2009, associated with changes in climate and atmospheric $CO_2$ concentration, for three land regions (northern land, tropical land, and southern land) and seven ocean regions (North Pacific, equatorial Pacific, South Pacific, North Atlantic, equatorial/South Atlantic, Indian Ocean, and Southern Ocean) (Fig. 1). The second aim is to determine which factors and processes among those included in the models are driving the modelled/observed trends in the regional land/ocean to atmosphere net $CO_2$ fluxes. For the land models, those factors and processes included are the $CO_2$ fertilisation effect on productivity and storage, as well as climate effects on productivity, respiration, and climate-caused natural disturbances (see Table S1 in the Supplement for details represented in individual models). A particular focus is on the impacts of climate variation and change on land ecosystems at the regional scale, as extreme climate events occurred during the period of 1990–2009 across many regions of the world, including North America (southwestern USA, 2000–2002), Europe (2003), Amazonia (2005), and eastern Australia (2001–2008), raising considerable attention in the ecological community regarding the consequences of recent climate variability on ecosystem structure and function (Allen et al., 2010) and the carbon cycle (Ciais et al., 2005; Van der Molen et al., 2011; Reichstein et al., 2013).

This study addresses the changes in the magnitude of the global carbon sink but does not discuss the efficiency of the sinks, which is widely discussed elsewhere (Raupach et al., 2014; Gloor et al., 2010; Ciais et al., 2013). These DGVMs have been extensively evaluated against observation-based gross primary production (GPP), land to atmosphere net $CO_2$ flux, and $CO_2$ sensitivity of net primary production (NPP) compared to results from free-air $CO_2$ enrichment (FACE) experiments (Piao et al., 2013).

Consideration of land use and land cover change (LULCC) on regional trends is beyond the scope of the present study, and therefore models assume a fixed present-day land use throughout the simulation period. Thus our results presented should be interpreted with this caveat in mind. There are large uncertainties in the global LULCC flux and its change through time, with an estimated decrease from $1.6 \pm 0.5$ Pg C yr$^{-1}$ (1990–1999) to $1.0 \pm 0.5$ Pg C yr$^{-1}$ (2000–2009) (LeQuéré et al., 2013). In addition, the net land use (LU) flux for the period 1990–2009 will be influenced by earlier LULCC (i.e. legacy fluxes), confounding the analysis. The response of the large fluxes associated with net primary productivity and heterotrophic respiration to climate variability and $CO_2$ are the focus of this study. Other companion papers investigate ecosystem response to interannual and seasonal timescales (Piao et al., 2013), and the carbon balance

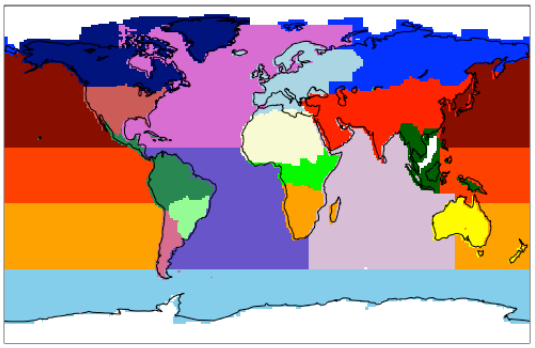

**Figure 1.** Land and ocean regions. The three land regions: northern land, tropical land, and southern land. Northern land comprises boreal North America (navy blue), Europe (light blue), boreal Asia (blue), temperate North America (pale red), and temperate Asia (red). Tropical land comprises tropical South American forests (sea green), northern Africa (sand), equatorial Africa (green), and tropical Asia (dark green). Southern land comprises South American savanna (pale green), temperate South America (violet), southern Africa (orange), and Australia and New Zealand (yellow). Ocean regions comprise North Pacific (dark red), equatorial Pacific (orange-red), South Pacific (orange), North Atlantic (orchid), equatorial/South Atlantic (slate blue), Indian Ocean (thistle), Southern Ocean (sky blue), and Arctic Ocean and Antarctica (white).

for individual land and ocean regions over the period 1990–2009 (see RECCAP special issue; Canadell et al., 2013, http://www.biogeosciences.net/special_issue107.html).

Trends and variability in the air–sea $CO_2$ fluxes simulated by the employed OBGCMs are driven by the increase in atmospheric $CO_2$ and by variability and change in ocean temperature, circulation, winds, and biology largely governed by climate variability. The air–sea $CO_2$ flux arising from the increase in atmospheric $CO_2$ is often referred to as the flux of anthropogenic $CO_2$, while the remainder, induced by changes in the natural cycling of carbon in the ocean–atmosphere system, is called the "natural" $CO_2$ component (e.g. Gruber et al., 2009). Although this conceptual separation has its limits (McNeill and Matear, 2013), it provides for a powerful way to understand how different forcings affect the net ocean sink.

DGVM results are compared with estimates of the residual land sink (RLS) and remote sensing products indicating trends of greening and browning in the northern region. Regional sources and sink trends are attributed to processes based on factorial simulations.

## 2 Methods

### 2.1 Dynamic global vegetation models

Following the studies of Le Quéré et al. (2009) and Sitch et al. (2008), a consortium of DGVM groups set up a project

to investigate further the spatial trends in land–atmosphere flux and agreed to perform a factorial set of DGVM simulations over the historical period, 1901–2009. These simulations have contributed to the RECCAP activity (Canadell et al., 2011, 2013). There are now a variety of DGVMs with origins in different research communities that typically contain alternative parameterisations and a diverse inclusion of processes (Prentice et al., 2007; Piao et al., 2013). DGVMs have emerged from the land surface modelling (LSM), forest ecology, global biogeography, and global biogeochemical modelling communities. Representative of these research strands are the following nine DGVMs, which are applied here: Hyland (Levy et al., 2004), JULES (Cox, 2001; Clark et al., 2011), LPJ (Sitch et al., 2003), LPJ-GUESS (Smith et al., 2001), NCAR-CLM4 (Thornton et al., 2007, 2009; Bonan and Levis, 2010; Lawrence et al., 2011), ORCHIDEE (Krinner et al., 2005), OCN (Zaehle and Friend, 2010), SDGVM (Woodward et al., 1995; Woodward and Lomas, 2004), and VEGAS (Zeng, 2003; Zeng et al., 2005). In this study we focus on two aspects of land surface modelling: the carbon and the hydrological cycles. In the case of land surface models coupled to GCMs, energy exchange between the land surface and atmosphere is also simulated.

### 2.2 Ocean biogeochemical general circulation models

A total of four different groups have conducted the factorial simulations over the analysis period with three-dimensional OBGCMs and submitted their results to the RECCAP archive. These are MICOM-HAMOCCv1 (BER) (Assmann et al., 2010), CCSM-WHOI using CCSM3.1 (BEC) (Doney et al., 2009a, b), CCSM-ETH using CCSM3.0 (ETH) (Graven et al., 2012), and NEMO-PlankTOM5 (UEA) (Buitenhuis et al., 2010). Details of the models are given in the respective publications cited and in Table 2. Not all model simulations are independent of each other, as several of them share components. BEC and ETH employ the same OBGCM, but differ in their spin-up and surface forcing. The employed models have relatively similar horizontal resolution of the order of 1 to 3° in longitude and latitude, i.e. none of them is eddy-permitting or eddy-resolving. The four ecosystem/biogeochemical models are also of comparable complexity, i.e. including explicit descriptions of at least one phytoplankton and zooplankton group, with some models considering up to three explicitly modelled groups for phytoplankton and two for zooplankton. All models use the same gas exchange parameterisation of Wanninkhof (1992), although with different parameters. In particular, the ETH model used a lower value for the gas exchange coefficient than originally used in the CCSM standard configuration, yielding a global-mean gas transfer velocity that is more than 25 % lower than those of the other models (Graven et al., 2012). This reduction reflects the mounting evidence based on radiocarbon analyses that the original global-mean gas transfer velocity of Broecker et al. (1985) was too high (Peacock, 2004; Sweeney et al., 2007; Müller et al., 2008).

### 2.3 Data sets

#### 2.3.1 Land

Climate forcing is based on a merged product of Climate Research Unit (CRU) observed monthly 0.5° climatology (v3.0, 1901–2009; New et al., 2000) and the high-temporal-resolution NCEP reanalysis. The merged product has a 0.5° spatial and 6 h temporal resolution. A coarse-resolution $3.75° \times 2.5°$ version at monthly timescales was also produced (see Table 1 for spatial resolution of individual DGVMs). Global atmospheric $CO_2$ was derived from ice core and NOAA monitoring station data, and provided at annual resolution over the period 1860–2009. As land use and land cover change was not simulated in these model experiments, models assume a constant land use (invariant agricultural coverage) throughout the simulation period. Atmospheric nitrogen deposition data for CLM4CN and OCN were sourced from Jean-Francois Lamarque (personal communication, 2012) and Dentener et al. (2006), respectively.

Gridded fields of leaf area index (LAI) are used in the evaluation of DGVM northern greening trends. These LAI data sets were based on remote sensing data and were generated from the AVHRR GIMMS NDVI3g product using an artificial neural network (ANN)-derived model (Zhu et al., 2013). The data set has a temporal resolution of 15 days over the period 1981–2011, and a spatial resolution of 1/12°.

#### 2.3.2 Ocean

Unlike how the land models simulations were set up, no common climatic forcing data set was used for the ocean model simulations. In fact, some models provided several simulation results obtained with different climatic forcings. Models were forced by the NCEP climatic data (Kalnay et al., 1996) in their original form, or in the modified CORE (Common Ocean-ice Reference Experiments – Corrected Normal Year Forcing (CORE-CNYF; Large and Yeager, 2004)) form (Table 2).

#### 2.3.3 Atmospheric inversion

Simulated trends in land to atmospheric net $CO_2$ flux are compared with those from version 11.2 of the $CO_2$ inversion product from the Monitoring Atmospheric Composition and Climate – Interim Implementation (MACC-II) service (http://copernicus-atmosphere.eu/). The horizontal resolution of the inversion is $3.75 \times 2.5$ square degrees (longitude $\times$ latitude), and weekly temporal resolution, with nighttime and daytime separated. The accuracy varies with the period and the location over the globe, depending on the density and the information content of the assimilated data, and usually decreases with increasing the resolution. Uncertainty

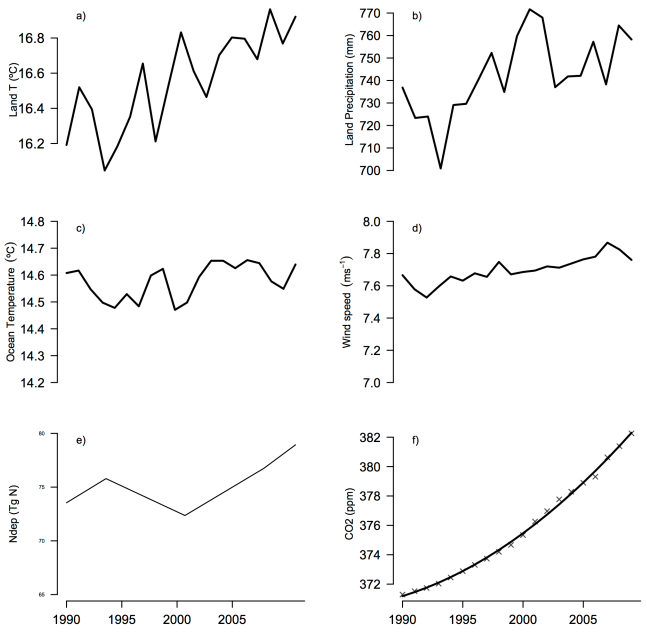


**Figure 2.** Global trends in environmental driving variables: **(a)** land temperature, **(b)** land precipitation, **(c)** ocean temperature, **(d)** wind speed, **(e)** N deposition, and **(f)** atmospheric [$CO_2$].

numbers at various scales can be found in Table 2 of Peylin et al. (2013). The inversion covers years 1979–2011, and a previous release has been documented by Chevallier et al. (2010). It uses a climatological prior without interannual variability, except for fossil fuel $CO_2$ emissions.

### 2.4 Experimental design

#### 2.4.1 Land

Model spin-up consisted of recycling climate mean and variability from the early decades of the 20th century (1901–1920) with 1860 atmospheric $CO_2$ concentration of 287.14 ppm until carbon pools and fluxes were in steady state (zero mean annual land to atmospheric net $CO_2$ flux). The land models were then forced over the 1861–1900 transient simulation using varying $CO_2$ and continued recycling of climate as in the spin-up. The land models were then forced over the 1901–2009 period with changing $CO_2$, climate, and fixed present-day land use according to the following simulations:

- S_L1: changing $CO_2$ only (i.e. time-invariant present-day land use mask, fixed pre-industrial climate);
- S_L2: changing $CO_2$ and climate (i.e. time-invariant present-day land use mask).

For DGVMs including the N cycle, N deposition was a time-variant forcing in both simulations, such that the difference between S_L2 and S_L1 includes the synergistic effects of N deposition on $CO_2$ fertilisation (Zaehle et al., 2010).

Figure 2 shows the historical changes in climate, atmospheric $CO_2$ concentration, and nitrogen deposition over the period 1990–2009 used to force the DGVMs. A summary of DGVM characteristics is given in Table 1. A more detailed description of DGVM process representations is given in Table S1.

#### 2.4.2 Ocean

The ocean models employed two different approaches for creating the initial conditions for the experiments. The first approach, followed by CCSM-ETH, CCSM-WHOI, and BER, involved first a multiple-century-long spin-up with climatological forcing and with atmospheric $CO_2$ held constant at its pre-industrial value, bringing these models very close to a climatological steady state for pre-industrial conditions (in some models $\sim$1750; in others $\sim$1850). In the second step, the models were then integrated forward in time through the historical period until 1948, with atmospheric $CO_2$ prescribed to follow the observed trend and a climatological forcing. The length of the spin-up varies from a few hundred years to several thousand years, resulting in differing global integrated drift fluxes, although their magnitudes are substantially smaller than 0.05 Pg C $yr^{-1}$ with essentially no rate of change. The second approach, followed by NEMO-PlankTOM5 (UEA), was to initialise the model with reconstructed initial conditions in 1920, and then also run it forward in time until 1948 with prescribed atmospheric $CO_2$, repeating the daily forcing conditions of a single year (1980). The modelled export production was tuned to obtain an ocean $CO_2$ sink of 2.2 Pg C $yr^{-1}$ in the 1990s. This second method offers the advantage that the model's carbon fields remain closer to the observations compared to the long spin-up approach, but it comes at the cost of generating a drift that affects the mean conditions and to a lesser extent the trend. Tests with the model runs of Le Quéré et al. (2010) suggest the drift in the mean $CO_2$ sink is about 0.5 Pg C $yr^{-1}$ and the drift in the trend is about 0.005 Pg C $yr^{-2}$ globally, and is largest in the Southern Ocean.

From $\sim$1950 onward, the models performed two separate simulations:

- S_O1: $CO_2$ only, i.e. atmospheric $CO_2$ increases, but models are forced with climatological atmospheric boundary conditions (referred to as ACO2 in the REC-CAP archive);
- S_O2: $CO_2$ and climate, i.e. as S_O1, but models are forced with "realistic" year-to-year variability in atmospheric boundary conditions (ANTH).

In these runs, both S_O1 and S_O2 are affected by the same drift, and their differences thus remove the drift. The CCSM-based models performed an additional experiment to better separate between the fluxes of natural and anthropogenic $CO_2$:

**Table 1.** Characteristics of the nine dynamic global vegetation models.

| Model name | Abbreviation | Spatial resolution | Land surface model | Full nitrogen cycle | River export flux | Fire simulation | Harvest/grazing flux | Source |
|---|---|---|---|---|---|---|---|---|
| Community Land Model 4CN | CLM4CN | $0.5° \times 0.5°$ | Yes | Yes | No | Yes | No | Oleson et al. (2010); Lawrence et al. (2011) |
| Hyland | HYL | $3.75° \times 2.5°$ | No | No | No | No | Yes | Friend et al. (1997); Levy et al. (2004) |
| Lund–Potsdam–Jena | LPJ | $0.5° \times 0.5°$ | No | No | No | Yes | Yes | Sitch et al. (2003) |
| LPJ-GUESS | LPJ-GUESS | $0.5° \times 0.5°$ | No | No | No | Yes | No | Smith et al. (2001) |
| ORCHIDEE-CN | OCN | $3.75° \times 2.5°$ | Yes | Yes | No | No | Yes | Zaehle and Friend (2010); Zaehle et al. (2010) |
| ORCHIDEE | ORC | $0.5° \times 0.5°$ | Yes | No | No | No | No | Krinner et al. (2005) |
| Sheffield-DGVM | SDGVM | $3.75° \times 2.5°$ | No | No | Yes | Yes | No | Woodward et al. (1995) |
| TRIFFID | TRI | $3.75° \times 2.5°$ | Yes | No | No | No | No | Cox (2001) |
| VEGAS | VEGAS | $0.5° \times 0.5°$ | Yes | No | Yes | Yes | Yes | Zeng et al. (2005) |

**Table 2.** Characteristics of the four ocean biogeochemical general circulation models (OBGCMs). All include NPZD-type ecosystem models and N, P, Si, and Fe nutrient components.

| Model name | Abbreviation | Spatial resolution | Meteorological forcing | Gas transfer formulation | Years used | Source |
|---|---|---|---|---|---|---|
| MICOM-HAMOCCv1 | BER | $2.4° \times 0.8-2.4°$ | NCEP | Wanninkhof (1992) | 1990 to 2009 | Assmann et al. (2010) |
| CCSM-WHOI | BEC | $3.6° \times 0.8-1.8°$ | NCEP | Wanninkhof (1992) | 1990 to 2009 | Doney et al. (2009a, b) |
| CCSM-ETH | ETH | $3.6° \times 0.9 \times 1.9°$ | CORE | Wanninkhof (1992) | 1990 to 2007 | Graven et al. (2012) |
| NEMO-PlankTOM5 | UEA | $2° \times 0.5-2°$ | NCEP | Wanninkhof (1992) | 1990 to 2009 | Buitenhuis et al. (2010) |

– S_O3: pre-industrial $CO_2$ and climate, i.e. atmospheric $CO_2$ is fixed at its pre-industrial level, but atmospheric boundary conditions vary as in S_O2 (PIND).

From these simulations, only the results from 1990 through to 2009 were analysed. Only the UEA and CCSM-WHOI models made results available for the S_O1 and S_O2 simulations for the entire analysis time. The results for the BER model for 2009 are incomplete, and the CCSM-ETH simulations extend only to 2007. In order to maintain a sufficiently large set of models, we decided to focus our analysis primarily on the 1990–2004 period, but occasionally also include the results through to 2009, with the important caveat that the latter are based only on two models.

### 2.5 Output variables

#### 2.5.1 Land

In this study we focus primarily on the simulated carbon cycle variables, net NPP, RH (heterotrophic respiration), and LAI, a measure of vegetation greenness. The land to atmosphere net $CO_2$ flux is

$$\text{land to atmosphere net}\,CO_2\,\text{flux} = -\text{NBP}$$
$$= \text{RH} + \text{wildfire flux riverine C flux} + \text{harvest} - \text{NPP},$$

where we have adopted the atmospheric perspective with regard to the sign of the fluxes, i.e. negative numbers indicate a sink for atmospheric $CO_2$ and a negative trend indicates an increasing sink or a decreasing source.

DGVMs typically do not represent all these processes; a list for each individual DGVM is given in Table 1. DGVM results for simulation S_L2 are compared against the global RLS, calculated as the annual anthropogenic $CO_2$ emissions (fossil fuel, cement manufacture, and land use C flux) minus the annual $CO_2$ growth rate and model mean ocean C sink as given by Friedlingstein et al. (2010). The ocean uptake is from the same OGGCMs as the ones used here, and the land use C flux is based on a book-keeping approach from Houghton (2010). Note the RLS depends on a LULCC model of emissions (the one of Houghton). Strictly speaking, comparison of model land to atmosphere net $CO_2$ flux with RLS is therefore inconsistent because these models treat areas affected by LUC as pristine ecosystems, and these areas are generally associated with a high land carbon sinks. Simulated net carbon flux from S2 is therefore likely to overestimate the RLS sink, by construction.

The regional analysis will focus on three large land regions (Fig. 1), and within these regions, trends at a finer spatial resolution, from multi-grid-cell to the sub-region, are analysed.

The comparison of DGVM simulated trends in the northern growing season against satellite-derived NDVI (normalised difference vegetation index) observations was based on eight models (JULES, LPJ, LPJ-GUESS, NCAR-CLM4, ORCHIDEE, OCN, SDGVM, VEGAS), which provided LAI outputs. The means and trends in the onset, end, and length of growing season were computed. Growing season variables were calculated using the methodology of Murray-Tortarolo et al. (2013). Leaf onset is defined as the day when LAI begins to increase above a critical threshold (CT), defined as

$$\text{CT} = \text{LAI}_{\text{min}} + 0.2 \cdot (\text{LAI}_{\text{max}} - \text{LAI}_{\text{min}}),$$

where $LAI_{min}$ and $LAI_{max}$ represent the minimum and maximum LAI over the annual cycle. Similarly, leaf senescence, or offset, or end of growing season, is defined as the day when LAI decreases below the CT. The length of the growing season in days is calculated as the end minus the onset. This calculation was made for each grid cell above 30° N (i.e. northern extratropics) from the models and the satellite data. In addition, any grid cell where LAI varied by less than 0.5 over the annual cycle from the satellite data was considered to be predominantly evergreen (e.g. boreal forest), and thus excluded from the analysis. We also masked out regions where LAI decreases in the summer (drought deciduous vegetation). In addition, when the growing season spans over the end of year (e.g. Mediterranean and some pixels particularly on the southern margin of the domain), we include the first 3 months of the second year in our analysis. Means and trends were calculated using a linear model over the period 1990–2009.

#### 2.5.2 Ocean

The modelling groups provided output on a monthly basis for the years 1990 through to 2004 and 2009 at two levels of priority. Tier-one data included the surface ocean fields of the air–sea $CO_2$ flux, oceanic $pCO_2$, dissolved inorganic carbon (DIC), alkalinity (Alk), temperature ($T$), salinity ($S$), and mixed layer depth. The second-tier data included the biological export at 100 m, the vertically integrated net primary production, and the surface chlorophyll $a$ concentration. Some models also supplied three-dimensional climatological fields of DIC, Alk, $T$, and $S$.

To determine the different factors contributing to the modelled trends and variations, we undertook two (linear) separations:

- The contribution of climate variability and change on the ocean carbon cycle: $X\_\mathrm{var} = X(\mathrm{S\_O2}) - X(\mathrm{S\_O1})$, $X$ is any variable or flux, where the expression in parentheses represents the results of the corresponding simulation, and $X$_var represents the impact of climate change and variability on the ocean carbon cycle.
- The contribution of anthropogenic $CO_2$: $X\_\mathrm{ant} = X(\mathrm{S\_O2}) - X(\mathrm{S\_O3})$.

For each of the integrations, but particularly for the changing $CO_2$ and climate simulation S_O2, we analysed the factors contributing to the temporal change in the air–sea $CO_2$ flux $F$ by a linear Taylor expansion (see e.g. Lovenduski et al., 2007 and Doney et al., 2009a):

$$\Delta F = \partial F/\partial \mathrm{ws} \cdot \Delta \mathrm{ws} + \partial F/\partial T \cdot \Delta T + \partial F/\partial \mathrm{ice} \cdot \Delta \mathrm{ice} + \partial F/\partial \mathrm{sDIC} \cdot \Delta \mathrm{sDIC} + \partial F/\partial \mathrm{sAlk} \cdot \Delta \mathrm{sAlk} + \partial F/\partial \mathrm{FS} \cdot \Delta S,$$

where ws is the wind speed, ice is the sea-ice fraction, sDIC and sAlk are the salinity normalised DIC and Alk concentrations, and $\partial F/\partial \mathrm{FS}$ is the change in the air–sea $CO_2$ flux in response to freshwater fluxes. This latter term includes not only the sensitivity of oceanic $pCO_2$ to changes in salinity but also the dilution effects of freshwater on DIC and Alk (see Doney et al., 2009a, for details). The partial derivatives were computed directly from the model equations for the mean conditions in each region. The changes in the driving components were derived from the trend computed via a linear regression of the model results and then multiplied by the length of the time series.

## 3 Results

### 3.1 Global Trends

#### 3.1.1 Land

The ensemble mean global land to atmosphere net carbon dioxide flux from S_L2 is $-2.38 \pm 0.72\,\mathrm{Pg\,C\,yr^{-1}}$ over the period 1990–2009 ($P = 0.04$, where $P$ is the probability of a trend statistically indistinguishable from zero; a significance level of 0.05 is selected) (Fig. 3, Fig. S1 in the Supplement, Table 3). The numbers behind ± signs are the 1 standard deviation of 20-year means for nine DGVMs. This compares to the global RLS of $-2.45 \pm 1.17\,\mathrm{Pg\,C\,yr^{-1}}$, inferred from the global carbon budget by Friedlingstein et al. (2010) over the same period. All DGVMs agree on an increasing land sink with a net flux trend over this period ranging between $-0.02$ and $-0.11\,\mathrm{Pg\,C\,yr^{-2}}$, corresponding to the OCN and Hyland DGVMs, respectively (Table 3). DGVMs simulate an increase in the land C sink with an ensemble mean trend of $-0.06 \pm 0.03\,\mathrm{Pg\,C\,yr^{-2}}$ ($P < 0.05$) over the period 1990–2009 (Table 3) in response to changes in climate and atmospheric $CO_2$ content. The two DGVMs with a fully coupled carbon and nitrogen cycle (CN) also simulate an increase in the land sink, at $-0.02$ ($P = 0.6$) for OCN and $-0.05\,\mathrm{Pg\,C\,yr^{-2}}$ ($P = 0.06$) for CLM4CN. DGVMs suggest the increase in global land sink between 1990 and 2009 is driven by increases in simulated global NPP (Fig. 3).

DGVMs simulate an ensemble mean global NPP of $62.9 \pm 8.73\,\mathrm{Pg\,C\,yr^{-1}}$ over the period 1990–2009 (Table 3). All DGVMs simulate an increase in NPP over this period, with an ensemble mean DGVM trend in NPP of $0.22 \pm 0.08\,\mathrm{Pg\,C\,yr^{-2}}$ ($P = 0.00$) (Table 3). Models with a higher NPP trend also produce a higher land to atmosphere net $CO_2$ flux trend (Fig. S2 in the Supplement). The ensemble mean NPP trend of $0.22 \pm 0.08\,\mathrm{Pg\,C\,yr^{-2}}$ ($P < 0.01$) from simulation S_L2 ($CO_2$ and climate forcing) contrasts with an ensemble trend of $0.19 \pm 0.08\,\mathrm{Pg\,C\,yr^{-2}}$ ($P < 0.01$) and $0.03 \pm 0.05\,\mathrm{Pg\,C\,yr^{-2}}$ ($P = 0.24$) over the same period for the S_L1 ($CO_2$ only) and S_L2–S_L1 (the climate effect), respectively (Tables S2, S3 in the Supplement). These results suggest that the simulated increase in global NPP is mainly in response to increasing atmospheric $CO_2$ (direct

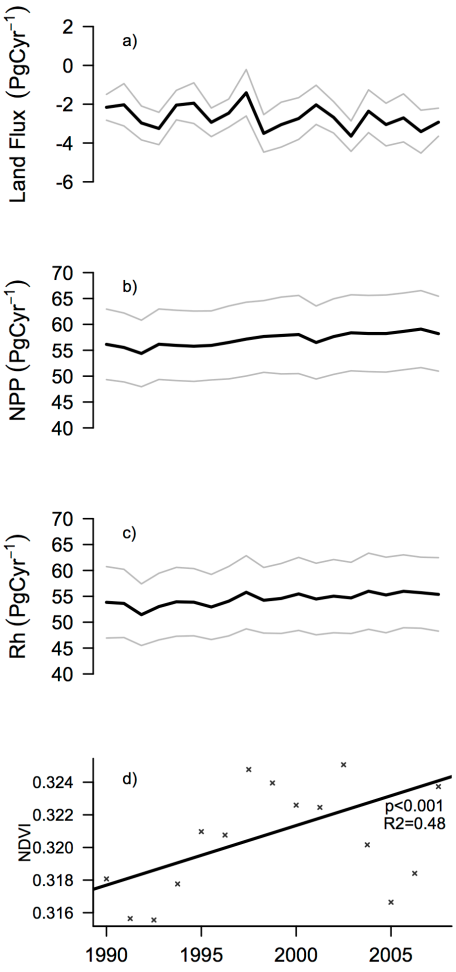


**Figure 3.** Global trends in ensemble land model responses. **(a)** DGVM mean model land to atmosphere net $CO_2$ flux and standard deviation (grey lines); (**b**) component fluxes, NPP; and (**c**) RH (= RH + wildfire + riverine C flux); and (**d**) remotely sensed trends in annual mean NDVI (crosses), a measure of vegetation greenness, and a linear regression through the data points (bold line).

$CO_2$ fertilisation of photosynthesis, in addition to the indirect benefits from an improved water balance in water-limited ecosystems due to the physiological effects of $CO_2$ on water use efficiency). VEGAS, CLM4CN, and OCN simulate the smallest positive trends in NPP among the DGVMs in response to elevated $CO_2$ forcing (Table S2). This suggests that the potential $CO_2$ fertilisation effect may be already strongly limited by present-day nitrogen availability in some ecosystems (Vitousek and Howarth, 1991). There is more uncertainty among models on the impact of climate changes on global NPP, with only two models simulating a significant positive trend (Table S3).

DGVMs simulate an ensemble mean global RH of $57.5 \pm 9.8$ Pg C yr$^{-1}$ over the period 1990–2009 (Table 3). All DGVMs simulate an increase in RH for S_L2 ($CO_2$ and climate), with an ensemble mean trend of

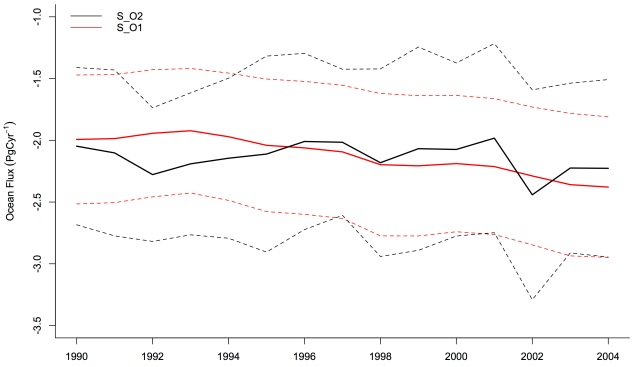


**Figure 4.** Global trends in ensemble ocean model fluxes. Black line: results from simulation S_O2 with variable "climate" and increasing $CO_2$. Red line: results from simulation S_O1 with constant "climate" and increasing $CO_2$. The dashed grey and dashed red lines indicate the ± uncertainty bands given by the four models that contribute to the ensemble mean.

$0.16 \pm 0.05$ Pg C yr$^{-2}$ ($P < 0.01$) over the period 1990–2009 (Table 3). This is lower than the trend in global NPP, resulting in a trend towards increasing net land carbon uptake. This is unsurprising as there is a lagged response in increases in RH relative to NPP, reflecting the turnover time of the newly incorporated plant material. The ensemble mean trend in RH is $0.12 \pm 0.06$ Pg C yr$^{-2}$ ($P < 0.01$) and $0.04 \pm 0.02$ Pg C yr$^{-2}$ ($P = 0.09$) over the same period for the S_L1 ($CO_2$ only) and S_L2–S_L1 (the climate effect), respectively (Tables S2, S3). This implies the dominant effect on RH is increased substrate for microbial respiration, with the additional litter input into soils, as a consequence of enhanced NPP, rather than enhanced rates of microbial decomposition with rising temperatures. Nevertheless, the simulated mean residence time (MRT = soil carbon / RH) of soil organic matter decreases, in response to warming, which is especially pronounced in high-latitude regions (Fig. S3 in the Supplement). The difference in land–atmosphere flux trend between the CN models OCN ($-0.02$ Pg C yr$^{-2}$) and CLM4CN ($-0.05$ Pg C yr$^{-2}$) is largely due their difference in RH trends at 0.14 and 0.11 Pg C yr$^{-2}$, respectively, rather than differential responses of simulated NPP to elevated $CO_2$ (Table 3).

Only four DGVMs simulated wildfire fluxes (CLM4CN, LPJ, LPJ-GUESS, SDGVM). No significant trends in the global wildfire flux were reported by any of the DGVMs.

### 3.1.2 Ocean

The global ocean is simulated to have acted as a very substantial sink for atmospheric $CO_2$ but one that has increased only slightly over the last two decades (see also discussion in Wanninkhof et al., 2013). The mean ocean sink in the four models (CCSM-ETH, CCSM-WHOI, UEA, and BER) increased from $\sim -2.0$ Pg C yr$^{-1}$ in the early 1990s to

$\sim -2.1\,\mathrm{Pg\,C\,yr^{-1}}$ during the first 5 years of the 21st century (Fig. 4).

We separate the mean and variable components by using our factorial experiments, i.e. by using S_O1 results to identify the ocean uptake in the absence of climate variability and change, and the difference between S_O2 and S_O1 as measure of the impact of climate change. This separation reveals that, in the absence of climate variability and change, the global ocean uptake would have increased from about $-1.98 \pm 0.04\,\mathrm{Pg\,C\,yr^{-1}}$ for the 1990–1994 period to $-2.3 \pm 0.09\,\mathrm{Pg\,C\,yr^{-1}}$ for 2000–2004 (for the two models that provided S_O1 results up to 2009 (CCSM-WHOI and UEA), the uptake flux would have increased from $-1.99$ to $-2.56\,\mathrm{Pg\,C\,yr^{-1}}$ for 2005–2009). This global net uptake flux and its substantial trend in time ($-0.03\,\mathrm{Pg\,C\,yr^{-2}}$ for 1990–2004, and $-0.04\,\mathrm{Pg\,C\,yr^{-2}}$ for 1990–2010) is entirely driven by the increase in atmospheric $CO_2$ and is – integrated globally – numerically equivalent to the ocean uptake flux of anthropogenic $CO_2$. Climate variability and change modified these fluxes, and particularly the trend in these models. The four models suggest an enhancement of the uptake in the early 1990s (1990–1994) of about $-0.2\,\mathrm{Pg\,C\,yr^{-1}}$, turning into a reduction of the uptake in the subsequent period (1995–1999), followed by a further reduction in the 2000–2004 period of $\sim +0.1\,\mathrm{Pg\,C\,yr^{-1}}$. This trend toward reduced uptake in response to climate variability and change of $+0.03\,\mathrm{Pg\,C\,yr^{-2}}$ nearly completely compensates for the anthropogenic $CO_2$ driven increase in uptake, causing the overall uptake of $CO_2$ to have a nearly flat trend over the 1990–2004 period of $< 0.01\,\mathrm{Pg\,C\,yr^{-2}}$ The same tendencies are found for the two models that extend over the entire 1990–2009 period: in these models, climate change and variability reduces the $CO_2$-driven trend of $-0.04\,\mathrm{Pg\,C\,yr^{-2}}$ by more than $+0.02\,\mathrm{Pg\,C\,yr^{-2}}$, to around $-0.02\,\mathrm{Pg\,C\,yr^{-2}}$.

With consideration of the different factors affecting the ocean carbon sink following our Taylor expansion, we find increasing sea surface temperature to be a globally important driver for the positive trends (reduced sinks) induced by climate change and variability. Over the 1990–2004 period, the surface ocean warmed, on average, by $0.004\,^{\circ}\mathrm{C\,yr^{-1}}$ ($0.005\,^{\circ}\mathrm{C\,yr^{-1}}$ from 1990 through to 2009). Isochemically, this leads to an increase in the oceanic $pCO_2$ of $\sim 0.06\,\mu\mathrm{atm\,yr^{-1}}$, which appears small. However, it needs to be compared with the trend in the global-mean air–sea $pCO_2$ difference of about $\sim 0.1\,\mu\mathrm{atm\,yr^{-1}}$ that is required in order to generate a trend in the ocean uptake of $-0.03\,\mathrm{Pg\,C\,yr^{-2}}$ (see e.g. Matsumoto and Gruber, 2005; Sarmiento and Gruber, 2006). The overall sink is therefore largely a consequence of the increase in atmospheric $CO_2$ (i.e. it mostly corresponds to the uptake flux of anthropogenic $CO_2$), but it includes a substantial perturbation flux stemming from the impact of climate variability and change on the ocean carbon cycle.

### 3.2 Regional trends

#### 3.2.1 Land

**Northern land**

All DGVMs agree on a land C sink over the northern land region, with a mean land–atmosphere flux of $-1.03 \pm 0.30\,\mathrm{Pg\,C\,yr^{-1}}$ over the period 1990–2009 (Fig. S4 in the Supplement, Table 3). The ensemble mean land–atmosphere flux trend is near zero for this region between 1990 and 2009 (Fig. S5 in the Supplement). Of particular interest are sub-regions with a simulated positive land–atmosphere flux trend (Fig. 5), implying a diminishing sink of atmospheric $CO_2$ or an increasing source of $CO_2$ to the atmosphere. At least six models out of nine agree on a decreasing regional land sink across some areas in temperate North America, eastern Europe, northeastern China, and Mongolia (Fig. 5). These largely correspond to regions with negative trends in precipitation (Fig. 6).

Over the northern region, which covers almost 50 % of the land surface, DGVMs simulate an ensemble mean NPP of $24.1 \pm 4.48\,\mathrm{Pg\,C\,yr^{-1}}$, which represents almost 40 % of the global total (Table 3). All DGVMs simulate an increase in northern NPP over this period, with a trend in NPP of $0.06 \pm 0.02\,\mathrm{Pg\,C\,yr^{-2}}$ ($P < 0.01$) (Table 3). However, enhanced productivity in the northern land region accounts for only around 29 % of the simulated global trend in NPP. The ensemble mean NPP trend of $0.06 \pm 0.02\,\mathrm{Pg\,C\,yr^{-2}}$ ($P < 0.01$) from simulation S2 ($CO_2$ and climate forcing) compares to a trend of $0.07 \pm 0.03\,\mathrm{Pg\,C\,yr^{-2}}$ ($P < 0.01$) and $-0.00 \pm 0.04\,\mathrm{Pg\,C\,yr^{-2}}$ ($P = 0.85$) for the S_L1 ($CO_2$ only) and S_L2–S_L1 (the climate effect), respectively (Tables S2, S3). All DGVMs simulate a positive trend in NPP in response to elevated $CO_2$ across the northern land region, and trends are all significant at the 95 % confidence level with the exception of CLM4CN ($P = 0.21$).

Large areas in temperate North America and Asia experienced warming combined with reductions in precipitation over the period 1990–2009 (Fig. 5). Indeed, although DGVMs simulate larger mean NPP in temperate compared to boreal regions (Table S5 in the Supplement), they simulate significant positive trends in boreal North America and boreal Asia, whereas trends in both temperate North America and Asia are smaller and not significant at the 95 % confidence level (Table S5).

In response to warming, models simulate an earlier onset (ensemble mean model trend $= -0.078 \pm 0.131\,\mathrm{days\,yr^{-1}}$) and delayed termination of the growing season ($0.217 \pm 0.097\,\mathrm{days\,yr^{-1}}$) based on LAI, and thus a trend towards a longer growing season in the northern extratropics ($0.295 \pm 0.228\,\mathrm{days\,yr^{-1}}$) (Fig. 7). This is in broad agreement with observed greening trends (Zhu et al., 2013; Murray-Tortarolo et al., 2013): onset $= -0.11\,\mathrm{days\,yr^{-1}}$, offset $= 0.252\,\mathrm{days\,yr^{-1}}$, and

**Table 3.** Mean and trends in NPP, RH, and land–atmosphere flux as simulated by individual DGVMs and the ensemble mean.

| MODEL | NPP ($Pg\,C\,yr^{-1}$) | Trend ($Pg\,C\,yr^{-2}$) | *P* value | RH ($Pg\,C\,yr^{-1}$) | Trend ($Pg\,C\,yr^{-2}$) | *P* value | Land–atm $CO_2$ flux ($Pg\,C\,yr^{-1}$) | Trend ($Pg\,C\,yr^{-1}$) | *P* value |
|---|---|---|---|---|---|---|---|---|---|
| Global_Land | | | | | | | | | |
| CLM4CN | 51.508 | 0.148 | 0.000 | 47.668 | 0.106 | 0.000 | −1.459 | −0.052 | 0.059 |
| HYLAND | 73.422 | 0.319 | 0.000 | 68.835 | 0.203 | 0.000 | −3.466 | −0.109 | 0.000 |
| LPJ | 59.306 | 0.216 | 0.000 | 47.612 | 0.117 | 0.000 | −2.251 | −0.068 | 0.061 |
| LPJ-GUESS | 62.506 | 0.174 | 0.000 | 55.448 | 0.145 | 0.000 | −1.802 | −0.043 | 0.346 |
| OCN | 53.941 | 0.155 | 0.000 | 50.611 | 0.135 | 0.000 | −2.272 | −0.015 | 0.568 |
| ORCHIDEE | 75.516 | 0.293 | 0.000 | 72.037 | 0.208 | 0.000 | −3.479 | −0.086 | 0.046 |
| SDGVM | 60.965 | 0.240 | 0.000 | 53.778 | 0.190 | 0.000 | −2.127 | −0.044 | 0.170 |
| TRIFFID | 71.929 | 0.305 | 0.000 | 69.167 | 0.244 | 0.000 | −2.762 | −0.061 | 0.265 |
| VEGAS | 57.308 | 0.113 | 0.006 | 51.930 | 0.092 | 0.000 | −1.783 | −0.018 | 0.551 |
| Ensemble | **62.934** | **0.218** | **0.000** | **57.454** | **0.160** | **0.000** | **−2.378** | **−0.055** | **0.048** |
| SD | **8.729** | **0.076** | | **9.791** | **0.053** | | **0.721** | **0.030** | |
| Northern_Land | | | | | | | | | |
| CLM4CN | 17.523 | 0.043 | 0.003 | 16.215 | 0.036 | 0.000 | −0.670 | −0.007 | 0.612 |
| HYLAND | 19.139 | 0.098 | 0.000 | 17.591 | 0.080 | 0.000 | −0.876 | −0.014 | 0.311 |
| LPJ | 24.566 | 0.079 | 0.001 | 19.578 | 0.062 | 0.006 | −1.168 | −0.006 | 0.735 |
| LPJ-GUESS | 28.484 | 0.039 | 0.085 | 25.883 | 0.067 | 0.009 | −0.634 | 0.023 | 0.521 |
| OCN | 21.008 | 0.044 | 0.035 | 19.264 | 0.047 | 0.008 | −1.117 | 0.007 | 0.632 |
| ORCHIDEE | 30.337 | 0.070 | 0.007 | 29.112 | 0.063 | 0.000 | −1.226 | −0.006 | 0.740 |
| SDGVM | 25.144 | 0.063 | 0.006 | 22.598 | 0.065 | 0.006 | −0.828 | 0.004 | 0.762 |
| TRIFFID | 28.476 | 0.088 | 0.009 | 27.006 | 0.103 | 0.001 | −1.470 | 0.016 | 0.455 |
| VEGAS | 21.895 | 0.048 | 0.012 | 18.914 | 0.043 | 0.001 | −1.322 | −0.000 | 0.968 |
| Ensemble | **24.064** | **0.063** | **0.001** | **21.796** | **0.063** | **0.001** | **−1.034** | **0.002** | **0.865** |
| SD | **4.484** | **0.022** | | **4.562** | **0.020** | | **0.295** | **0.012** | |
| Tropical_Land | | | | | | | | | |
| CLM4CN | 26.400 | 0.090 | 0.000 | 24.464 | 0.058 | 0.000 | −0.692 | −0.039 | 0.110 |
| HYLAND | 34.489 | 0.112 | 0.000 | 32.695 | 0.067 | 0.000 | −1.560 | −0.044 | 0.001 |
| LPJ | 25.830 | 0.100 | 0.001 | 21.224 | 0.035 | 0.001 | −0.817 | −0.049 | 0.031 |
| LPJ-GUESS | 21.922 | 0.078 | 0.000 | 19.332 | 0.051 | 0.000 | −0.785 | −0.036 | 0.038 |
| OCN | 22.750 | 0.084 | 0.000 | 21.476 | 0.065 | 0.000 | −0.982 | −0.017 | |
| ORCHIDEE | 31.313 | 0.151 | 0.000 | 29.640 | 0.108 | 0.000 | −1.673 | −0.043 | 0.084 |
| SDGVM | 23.505 | 0.118 | 0.000 | 20.677 | 0.075 | 0.000 | −0.984 | −0.038 | 0.030 |
| TRIFFID | 29.801 | 0.141 | 0.000 | 28.925 | 0.096 | 0.000 | −0.876 | −0.045 | 0.218 |
| VEGAS | 23.472 | 0.041 | 0.061 | 21.994 | 0.033 | 0.004 | −0.278 | −0.010 | 0.527 |
| Ensemble | **26.609** | **0.102** | **0.000** | **24.492** | **0.065** | **0.000** | **−0.961** | **−0.036** | **0.045** |
| SD | **4.350** | **0.034** | | **4.752** | **0.025** | | **0.428** | **0.013** | |
| Southern_Land | | | | | | | | | |
| CLM4CN | 7.617 | 0.014 | 0.187 | 7.017 | 0.011 | 0.036 | −0.098 | −0.005 | 0.719 |
| HYLAND | 19.875 | 0.109 | 0.000 | 18.623 | 0.056 | 0.000 | −1.035 | −0.051 | 0.000 |
| LPJ | 8.940 | 0.037 | 0.074 | 6.833 | 0.021 | 0.004 | −0.267 | −0.013 | 0.355 |
| LPJ-GUESS | 12.124 | 0.058 | 0.003 | 10.255 | 0.026 | 0.001 | −0.385 | −0.031 | 0.192 |
| OCN | 10.222 | 0.027 | 0.165 | 9.909 | 0.023 | 0.053 | −0.174 | −0.004 | 0.744 |
| ORCHIDEE | 13.884 | 0.073 | 0.002 | 13.304 | 0.037 | 0.000 | −0.581 | −0.036 | 0.027 |
| SDGVM | 12.358 | 0.059 | 0.034 | 10.539 | 0.050 | 0.000 | −0.317 | −0.010 | 0.701 |
| TRIFFID | 13.707 | 0.077 | 0.020 | 13.290 | 0.045 | 0.000 | −0.417 | −0.032 | 0.269 |
| VEGAS | 11.971 | 0.024 | 0.382 | 11.049 | 0.016 | 0.140 | −0.182 | −0.009 | 0.656 |
| Ensemble | **12.300** | **0.053** | **0.011** | **11.202** | **0.032** | **0.000** | **−0.384** | **−0.021** | **0.196** |
| SD | **3.528** | **0.031** | | **3.597** | **0.016** | | **0.285** | **0.017** | |

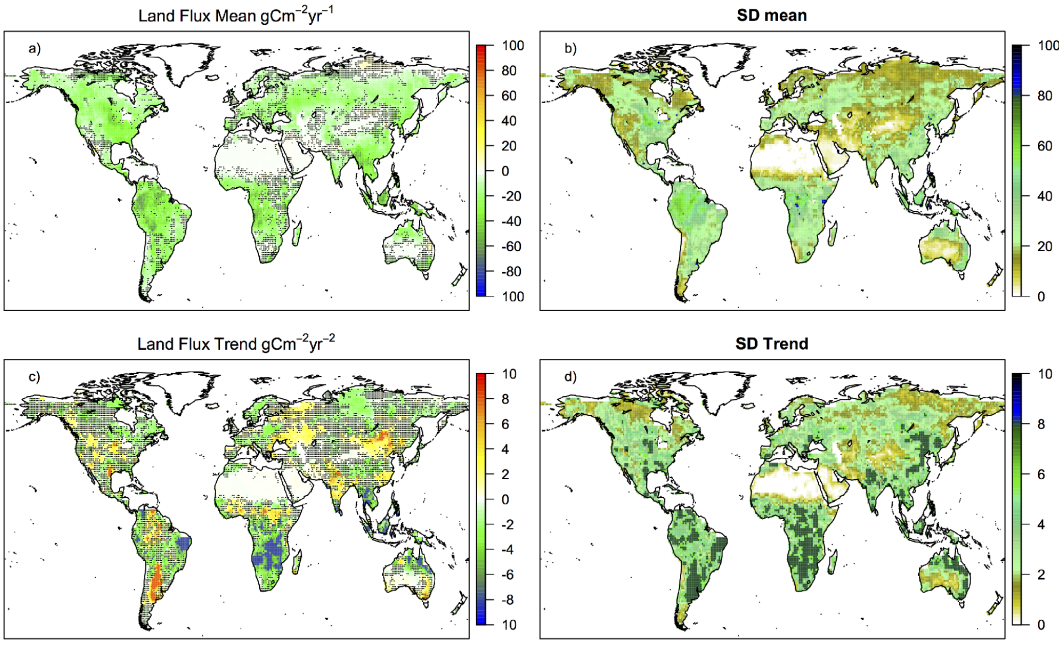


**Figure 5. (a)** Average land to atmosphere net $CO_2$ flux over the period 1990–2009 for the ensemble mean and model disagreement, with stippling representing agreement for < 66 % of DGVMs , and **(b)** standard deviation across DGVMs. **(c)** The trend in land to atmosphere net $CO_2$ flux across the ensemble, and model disagreement, with stippling representing agreement of < 66 % of the DGVMs , and **(d)** the standard deviation of the trend.

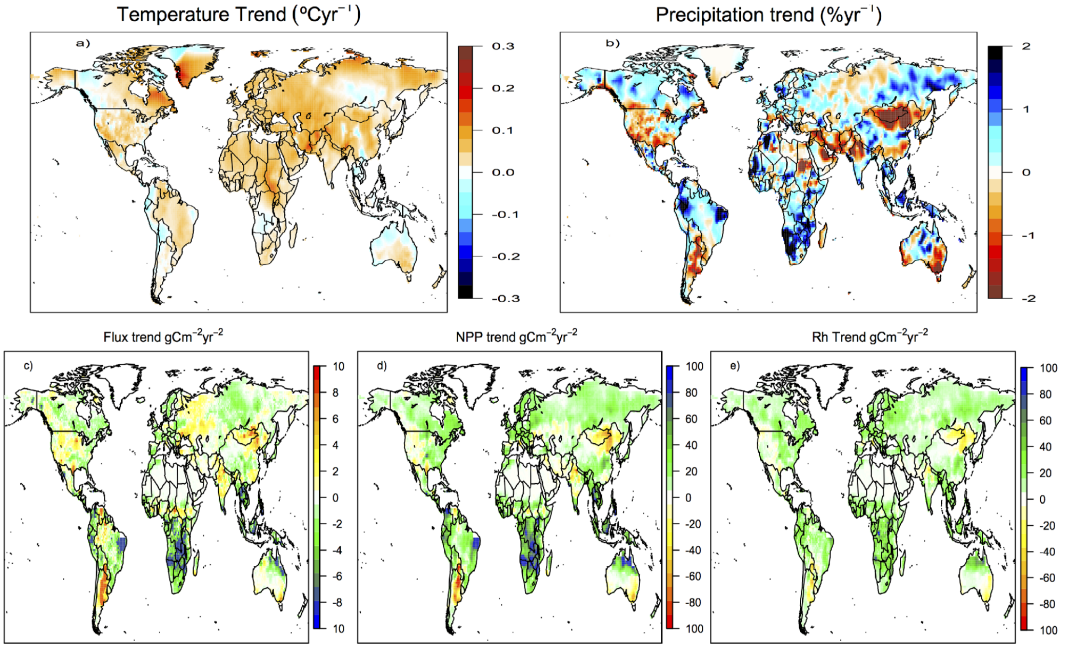


**Figure 6.** Trends in land climate drivers and process responses. **(a)** Trend in temperature (°C yr$^{-1}$), **(b)** trend in precipitation (% yr$^{-1}$), **(c)** trend in land to atmosphere net $CO_2$ flux (gC m$^{-2}$ yr$^{-2}$), **(d)** trend in NPP (gC m$^{-2}$ yr$^{-2}$), and **(e)** trend in RH (= RH + wildfire + Riverine C flux) (gC m$^{-2}$ yr$^{-2}$).

growing season length = 0.361 days yr$^{-1}$. There is less agreement among models on reproducing the observed browning trends in some regions of the boreal forest.

DGVMs simulate an ensemble mean RH of $21.8 \pm 4.6$ Pg C yr$^{-1}$ across the northern land region (Table 3). All DGVMs simulate an increase in northern RH over the period 1990–2009, with a significant trend in RH of $0.063 \pm 0.02$ Pg C yr$^{-1}$ ($P < 0.01$) (Table 3). DGVMs simulate larger mean RH in temperate compared to boreal regions, yet smaller positive trends for Asia (Table S6 in the Supplement). This is because of relatively smaller increases in substrate (i.e. NPP) in temperate regions and greater warming in boreal regions stimulating microbial decomposition, reducing mean residence time of carbon in soils (MRT = soil carbon / RH; see Fig. S3).

No significant trends in the wildfire flux were reported by any of the DGVMs for the northern land region. However, DGVMs agree on simulating a small negative trend in wildfire flux across boreal North America and tundra.

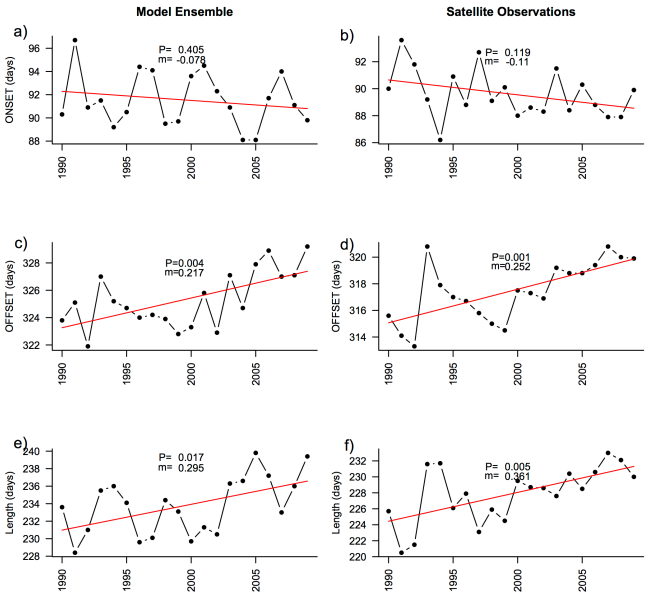


**Figure 7.** Ensemble-mean trends in the onset **(a, b)**, offset **(c, d)**, and length of growing season in days **(e, f)** for the ensemble mean (left) compared with satellite-derived estimates (right).

## Tropical land

All DGVMs simulate an increasing land C sink over recent decades, in response to changes in climate and atmospheric $CO_2$ concentration over the tropical land region, with an ensemble mean land–atmosphere flux of $-0.96 \pm 0.43$ Pg C yr$^{-1}$ (Table 3, Fig. S4) and trend of $-0.04 \pm 0.01$ Pg C yr$^{-2}$ ($P = 0.05$), or $-0.88 \pm 0.33$ g C m$^{-2}$ yr$^{-2}$ on an area basis (Table 3, Table S4 in the Supplement Fig. S5). This represents 65 % of the increase in global land sink over the last two decades across the tropical land, which covers 27 % of the land surface (Table S4). DGVMs simulate significant negative trends (i.e. increasing sinks) across tropical Asia and equatorial Africa (Table S4).

DGVMs simulate an ensemble mean NPP of $26.6 \pm 4.35$ Pg C yr$^{-1}$ averaged over the tropical region, representing 42 % of the global total (Table 3). All DGVMs simulate a significant increase in tropical NPP over this period, with an ensemble mean trend in NPP of $0.10 \pm 0.03$ Pg C yr$^{-2}$ ($P = 0.00$) for S_L2 (Table 3). This compares to a trend of $0.09 \pm 0.03$ Pg C yr$^{-2}$ ($P < 0.01$) and $0.02 \pm 0.02$ Pg C yr$^{-2}$ ($P = 0.33$) over the same period for the S_L1 ($CO_2$ only) and S_L2–S_L1 (the climate effect), respectively (Tables S2, S3). Again, the simulated trend in NPP is dominated by the simulated response of ecosystems to elevated atmospheric $CO_2$ content. DGVMs simulate positive NPP trends across tropical South American forests, tropical Asia, equatorial Africa, and North African savanna (Table S5). Nevertheless there are some areas within tropical South America and North African savanna regions with negative trends in NPP (Fig. 6).

All DGVMs simulate an increase in RH over the period 1990–2009, with an ensemble mean RH of $24.49 \pm 4.75$ Pg C yr$^{-1}$ (Table 3) and trend of $0.065 \pm 0.025$ Pg C yr$^{-2}$ ($P < 0.01$). This can be largely attributed to the response of ecosystems to elevated $CO_2$ (Table S2).

No significant trends in the wildfire flux were reported by any of the DGVMs for the tropical land region. However, DGVMs agree on simulating a negative trend in wildfire flux across equatorial Africa and tropical Asia.

## Southern land

All DGVMs agree on a net land sink over the southern land during the last two decades, with an ensemble mean land–atmosphere flux of $-0.38 \pm 0.29$ Pg C yr$^{-1}$ (Table 3, Fig. S4). Although all DGVMs simulate an increase in the land sink over the southern extratropics, with an ensemble mean land–atmosphere trend of $-0.02 \pm 0.02$ Pg C yr$^{-2}$ ($P = 0.20$) (Fig. S5) or $-0.58 \pm 0.45$ g C m$^{-2}$ yr$^{-2}$ on an area basis, only trends for HYL and ORC are significant at the 95 % confidence level (Table 3). Ensemble mean trends are significant for temperate South American and southern African regions at $0.005 \pm 0.005$ Pg C yr$^{-2}$ ($P = 0.05$) and $-0.022 \pm 0.011$ Pg C yr$^{-2}$ ($P = 0.01$), respectively (Table S4). For southern Africa, all DGVMs simulate an increase in the land sink in response to climate variability and change over this period (five out of nine are significant at the 90 % confidence level) (Table S7 in the Supplement, Fig. 6). In contrast, the simulated decrease in land sink for temperate South America is associated with a decrease in precipitation over 1990–2009 (Table S8 in the Supplement).

DGVMs simulate an ensemble mean NPP of $12.3 \pm 3.53$ Pg C yr$^{-1}$ over the southern extratropics,

which represents ∼20 % of the global total (Table 3) across 24 % of the land surface. All DGVMs simulate an increase in NPP over this period, with a significant ensemble mean trend of $0.05 \pm 0.03\,\mathrm{Pg\,C\,yr^{-2}}$ ($P = 0.01$), i.e. the southern land region accounts for around 25 % of the simulated global trend in NPP. Southern Africa is the only southern sub-region with a significant trend in NPP of $0.041 \pm 0.018\,\mathrm{Pg\,C\,yr^{-2}}$ ($P < 0.01$) (Table S5), due to a positive response of plant production to both $CO_2$ and climate, and is likely in response to increases in precipitation over the last two decades (Table S7, Fig. 5).

DGVMs simulate an ensemble mean RH of $11.20 \pm 3.60\,\mathrm{Pg\,C\,yr^{-1}}$ over the southern land region (Table 3). All DGVMs simulate an increase in RH over the period 1990–2009, with a significant trend in the ensemble mean RH of $0.03 \pm 0.02\,\mathrm{Pg\,C\,yr^{-2}}$ ($P < 0.01$). This is only partly explained by the response of ecosystems to elevated $CO_2$; over southern Africa the ensemble mean trend in RH from S_L1 is $0.01 \pm 0.01\,\mathrm{Pg\,C\,yr^{-2}}$ ($P < 0.01$), and a climate-induced positive trend in RH of $0.01 \pm 0.00\,\mathrm{Pg\,C\,yr^{-1}}$ ($P < 0.01$) (Table S2, S7).

No significant trends in the wildfire flux were reported by any of the DGVMs for the southern land region. However DGVMs agree on simulating a negative trend in wildfire flux across southern Africa.

In summary, the globally increasing trend in land carbon sink is about two-thirds due to tropical ecosystems and one-third due to the southern land region, with zero contribution from northern land. This partitioning in trend is quite different from the mean carbon sink fluxes themselves, which is more like 43 : 41 : 16 (northern : tropical : southern).

### Qualitative change in processes

A qualitative assessment of the differential responses of the underlying land processes to changes in environmental conditions, and their contribution to the sink–source land–atmosphere flux trends is shown in Fig. 8. Many regions are simulated to have a negative land–atmosphere flux trend, with increases in NPP leading increases in RH. However there are locations with positive trends over the period 1990–2009, i.e. red colours in Fig. 8. In some regions models simulate a positive trend in NPP but an even larger positive trend in RH (eastern Europe, southeastern USA, Amazonia, southern China, North America tundra). Warming is likely to enhance both NPP and RH in high-latitude ecosystems, but primarily RH in low latitudes. Reduced precipitation may partially or fully offset the benefits of elevated atmospheric $CO_2$ abundance on NPP, and the response of RH to changes in precipitation is not obvious, as this is influenced by the initial soil moisture status. This is because microbial activity increases with increasing soil moisture at low moisture levels, before reaching a maximum activity, and then begins to decline as water completely fills the soil pore spaces and oxygen becomes more limiting to respiration. Locations in the western USA, southern Asia, northern boreal China, southeastern South America, and western and southern Australia are simulated to have negative NPP trends over the last two decades, as a result of reduced rainfall, and there is a less negative trend in RH, possibly due to a reduction in microbial respiration rates with increased soil dryness. The warming and drying in central Asia (northeastern China and Mongolia) and southern Australia is simulated to reduce the rate of microbial decomposition in these regions (Fig. S3), which partly opposes the NPP-driven lagged decrease in RH. The source trend in eastern Europe is simulated as a combination of a negative trend in NPP, as a result of a combination of elevated temperatures and reduced precipitation (i.e. soil drying), and a positive trend in RH driven by increasing temperature, despite reduced plant litter input.

## .2 Ocean

### Regional fluxes

The large-scale distribution of the modelled mean surface fluxes consists of strong outgassing in the tropical regions, especially in the Pacific, and broad regions of uptake in the mid-latitudes, with a few regions in the high latitudes of particularly high uptake, such as the North Atlantic (Fig. 9). This pattern is largely the result of the exchange flux of natural $CO_2$ that balances globally to a near-zero flux, but exhibits regionally strong variations (Gruber et al., 2009). Superimposed on this natural $CO_2$ flux pattern is the uptake of anthropogenic $CO_2$, which is taken up everywhere, but with substantial regional variation. Large anthropogenic $CO_2$ uptake fluxes occur in the regions of surface ocean divergence, such as the equatorial Pacific and particularly the Southern Ocean (Sarmiento et al., 1992; Gloor et al., 2003; Mikaloff Fletcher et al., 2006). This is a result of the divergence causing waters to upwell to the surface which have not been exposed to the atmosphere for a while, thereby permitting them to take up a substantial amount of anthropogenic $CO_2$. This reduces the outgassing that typically characterises these regions as a result of these upwelling waters also bringing with them high carbon loads from the remineralisation of organic matter.

Over the analysis period, the air–sea $CO_2$ fluxes exhibit only a remarkably small trend in most places, with some regions increasing in uptake, while others show a positive flux anomaly, i.e. lesser uptake. Thus the small global trend in ocean uptake over the 1990–2004 analysis period is a result of also the individual regions having relatively modest trends.

### Process analysis

The regional flux trends are, however, much smaller than expected from an ocean with constant circulation that is only responding to increasing atmospheric $CO_2$, and hence would tend to increase its uptake of anthropogenic $CO_2$ through

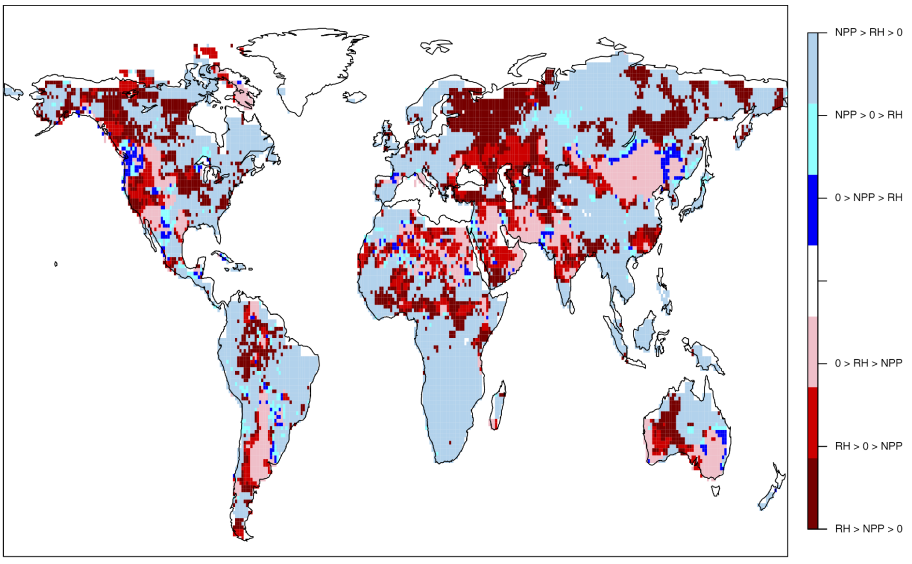


**Figure 8.** Qualitative change in processes over the period 1990–2009. Negative trend in land–atmosphere net $CO_2$ flux: enhanced NPP > enhanced RH (= RH + wildfire + riverine C flux) (pale blue); enhanced NPP, reduced RH (turquoise); and reduced NPP < reduced RH (dark blue). Positive trend in land–atmosphere net $CO_2$ flux: enhanced NPP < enhanced RH (dark red); reduced NPP, enhanced RH (red); and reduced NPP > reduced RH (pink).

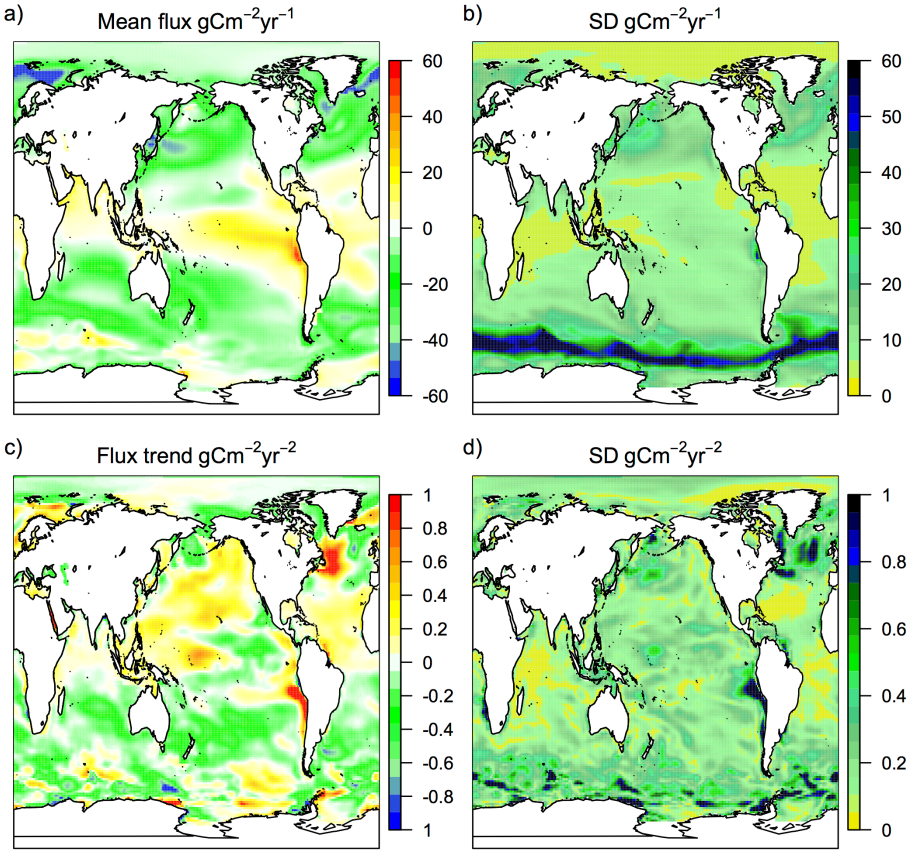


**Figure 9.** Gridded maps of the ensemble mean sea–air $CO_2$ flux over the period 1990–2004 **(a)**, standard deviation of the mean flux across the four OBGCMs **(b)**, the trend in the net flux across the ensemble **(c)**, and the standard deviation of the trend **(d)**.

time (Fig. 10). In the absence of climate variability and change, all regions would have flux density trends of more than $-0.05\,\mathrm{g\,C\,m^{-2}\,yr^{-2}}$, with some regions, such as the Southern Ocean, exceeding $-0.15\,\mathrm{g\,C\,m^{-2}\,yr^{-2}}$. However climate variability and change compensate for these negative trends in every single region by increasing them by $+0.04\,\mathrm{g\,C\,m^{-2}\,yr^{-2}}$ or more (with the exception of the South Pacific), such that the overall trends fluctuate from region to region around zero (Fig. 10). The largest reductions in trends are simulated to occur in the North and equatorial Pacific and in the North Atlantic, where they even cause a change in the sign of the overall trend. A similar, although slightly more moderate, pattern is seen if the analysis is undertaken for the entire 1990–2009 period with two models only. The most important difference is found in the North Atlantic, where the climate variability impact is substantially smaller, and not offsetting the anthropogenic $CO_2$ trend when analysed for 1990–2009.

The mechanisms driving the oceanic flux trends differ between the analysed regions. Attribution of regional trends to specific processes or changes in specific state variables in the different models is a work in progress, and is difficult to achieve with high confidence as yet. This is due to the antagonistic effect of ocean warming on $CO_2$ solubility and on dissociation of carbonic acid into bicarbonate and carbonate, as well as to the complex changes in ocean circulation and mixing, which themselves influence the biological carbon pumps of the ocean.

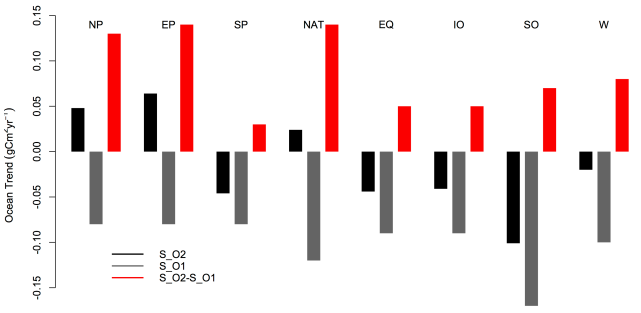


**Figure 10.** Regional ocean flux trends from 1990 through to 2004 for the standard case, i.e. variable climate and increasing $CO_2$ (simulation S_O2), and for the constant climate case (simulation S_O1), and their difference (S_O2–S_O1). Ocean regions comprise North Pacific (NP), equatorial Pacific (EP), South Pacific (SP), North Atlantic (NAT), equatorial/South Atlantic (EQ), Indian Ocean (IO), and Southern Ocean (SO), and world oceans (W).

## 4 Discussion

### 4.1 Land

The DGVMs used in this study simulate an increase in land carbon uptake over the period 1990–2009. The result is consistent with the earlier findings of Sarmiento et al. (2010), who suggested a large increase in the RLS between 1960 and 1988 and between 1989 and 2009 (Table S9 in the Supplement). The ensemble mean land–atmosphere flux increased by $-1.11\,\mathrm{Pg\,C\,yr^{-1}}$ for the same period, compared to the estimated RLS increase of $-0.88\,\mathrm{Pg\,C\,yr^{-1}}$ from Sarmiento et al. (2010). The DGVM ensemble trends in land uptake for the globe, northern, tropical, and southern land regions of $-0.06 \pm 0.03$, $0.00 \pm 0.01$, $-0.04 \pm 0.01$, and $-0.02 \pm 0.02\,\mathrm{Pg\,C\,yr^{-2}}$, respectively, compare favourably with the inversion estimates of $-0.06 \pm 0.04$, $-0.01 \pm 0.01$, $-0.04 \pm 0.02$, and $-0.01 \pm 0.01\,\mathrm{Pg\,C\,yr^{-2}}$ over the period 1990–2009. Although encouraging, these results should be interpreted with caution because the inversion accounts for any trend in the land use change flux over this period, whereas DGVMs had fixed land use.

There is empirical evidence of a large increase in biomass in intact forest in tropical South America and Africa (Pan et al., 2011; Baker et al., 2004; Lewis et al., 2009a, b), which is consistent with the DGVM projections presented here. Lewis et al. (2009b) found broad agreement between biomass trends from observations and from a suite of carbon cycle models applied with 20th century forcing of climate and atmospheric $CO_2$ content, using a similar protocol to the current analysis. DGVMs suggest a large component of the uptake trend is associated with a positive NPP response to elevated $CO_2$, which is broadly consistent with the enhancement of forest production due to $CO_2$ observed in FACE experiments (Norby et al., 2005), although they are largely located in temperate forest ecosystems. However, recent studies have highlighted the role of nitrogen in limiting the long-term $CO_2$ response (Canadell et al., 2007; Norby et al., 2010) in these ecosystems. The long-term plant response to elevated $CO_2$ is likely affected by nutrients and its impact on plant C allocation (Zaehle et al., 2014), however only two out of the nine models used here (CLM4CN and OCN) include interactive nutrient cycling (see DGVM characteristics, Table S1).

In contrast to the large trend in net C uptake across the tropics, DGVMs simulate no statistically significant trend over the northern land region. In particular, trends in NPP over temperate regions are smaller than those in boreal regions, and are also not significant. Many temperate areas experienced a decrease in rainfall between 1990 and 2009, and suffered periods of prolonged and severe drought. Examples include the drought in the western USA of 2000–2004 (McDowell et al., 2008; Anderreg et al., 2012) and the 2003 summer heatwave in Europe (Ciais et al., 2005). Zscheischler et al. (2014) suggest that negative productivity extremes dominated interannual variability in productivity during the period 1982–2011; these extremes are evident particularly over temperate latitudes.

Satellite observations suggest a general greening trend in high latitudes, with an earlier onset and longer growing season in high-latitude ecosystems, which is reproduced by the DGVMs. Observations suggest a greening tundra and a

slower greening and possible browning in some regions of the boreal forest (Tucker et al., 2001; Bhatt et al., 2010), especially in North America (Beck and Goetz, 2011). In tundra ecosystems, an earlier onset is attributed to warming and earlier snowmelt. In these ecosystems, the start of the growing season corresponds to near peak in radiation. Thus any temperature-induced earlier snowmelt (McDonald et al., 2004; Sitch et al., 2007a) is likely to enhance plant production. Warming may not have such a great effect on the end of the growing season in Arctic tundra ecosystems, as this may be driven primarily by radiation. DGVMs simulate a significant positive trend in NPP in boreal North America and boreal Asia and the circumpolar tundra. Nitrogen limitation is also likely to constrain the productivity at high latitudes, but it was not possible to quantify N-limitation effects on regional trends in this study.

DGVMs simulate decreasing NPP across northeastern China and Mongolia, contributing to the overall decreasing land uptake trend, in response to recent climate. In a regional study, Poulter et al. (2013) investigated the differential response of cool semi-arid ecosystems to recent warming and drying trends across Mongolia and northern China, using multiple sources of evidence, including the LPJ DGVM, FPAR remotely sensed data (derived from GIMMS NDVI3g), and tree-ring widths. They found coherent patterns of high sensitivity to precipitation across data sources, which showed some areas with warming-induced springtime greening and drought-induced summertime browning, and limitations to NPP explained mainly by soil moisture.

Browning has occurred as a consequence of regional drought, wildfire, and insect outbreak, and their interaction, especially in North America (Beck and Goetz, 2011). Disturbance plays a key role in the ecology of many global ecosystems. For example, wildfire plays a dominant role in the carbon balance of boreal forest in central Canada and other regions (Bond-Lamberty et al., 2007), and insect outbreaks like the mountain pine beetle epidemic between 2000 and 2006 in British Colombia, Canada, resulted in the transition of forests from a small carbon sink to a source (Kurz et al., 2008). In general, disturbance and forest management are inadequately represented by the current generation of DGVMs, even though several models include simple prognostic wildfire schemes (Table S1), while some are starting to include other disturbance types such as insect attacks (Jönsson et al., 2012) and windthrow (Lagergren et al., 2012). The extension of DGVMs to include representations of globally and regionally important disturbance types and their response to changing environmental conditions is a priority.

In Table 4, DGVM results are compared with the REC-CAP synthesis papers documenting carbon sources and sinks for individual regions. Note that DGVMs provided one source of evidence for some regional papers. Over Russia, DGVMs agree on a sink yet underestimate that sink's magnitude, likely related to soil respiration (which is unsurprising, as many DGVMs have a limited representation of permafrost and active layer thickness) (Dolman et al., 2012). In South America, DGVMs agree with inventory-based estimates on a sink in natural forests (Gloor et al., 2012). DGVMs also agree with other data sources on the sign and magnitude of the natural land sink over Australia (Harverd et al., 2013). Over Europe DGVMs simulate a smaller mean land sink than the synthesis study suggests (Luyssaert et al., 2012). However, the regional synthesis was conducted over the shorter time period 2001–2005. For the Arctic, DGVMs tend to simulate a lower sink than regional process-based models (McGuire et al., 2012). However, over the 1990–2006 period, DGVMs are in line with observations and inversions on the magnitude and sign of the natural land sink, and DGVM results also suggest a sink trend in line with observations. DGVMs simulate a land sink over South Asia in agreement with inversions; however there were limited data to compare trends from DGVMs and other products (Patra et al., 2013). For East Asia, DGVM results agree remarkably well with remote sensing model–data fusion and inverse models on the magnitude of the land sink over the period 1990–2009. Finally, for Africa, DGVMs are broadly consistent with inventory- and flux-based estimates in simulating a land sink over Africa, albeit of lower magnitude (Valentini et al., 2014).

### 4.2 Ocean

The investigated OBGCMs consistently simulate an ocean characterised by a substantial uptake of $CO_2$ from the atmosphere, but with a global integrated trend in the last two decades ($-0.02 \pm 0.01\,\mathrm{Pg\,C\,yr^{-2}}$) that is substantially smaller than that expected based on the increase in atmospheric $CO_2$. Results based on the predictions from ocean inversion and ocean Green function methods (Mikaloff Fletcher et al., 2006; Gruber et al., 2009; Khatiwala et al., 2009) suggest an increase in ocean uptake with a trend of the order of $-0.04\,\mathrm{Pg\,C\,yr^{-2}}$ over the analysis period (see also Wanninkhof et al., 2013). These latter methods assume constant circulation, while our simulations here include the impact of climate variability and change.

Our analyses reveal that recent climate variability and change has caused the ocean carbon cycle to take up less $CO_2$ from the atmosphere than expected on the basis of the increase in atmospheric $CO_2$, i.e. it reduces the efficiency of the ocean carbon sink. Globally, we find that this efficiency reduction is primarily a result of ocean warming, while, regionally, many more processes (e.g. wind changes, alkalinity/DIC concentration changes) are at play.

Is this reduction in uptake efficiency over the analysis period the first sign of a positive feedback between global warming and the ocean carbon cycle – or, alternatively, could it just reflect natural decadal-scale variability in air–sea $CO_2$ fluxes? Without a formal attribution study, it is not possible to provide a firm answer. We suspect that the majority of the trend in the efficiency is due to

**Table 4.** Ensemble DGVM regional NBP mean comparison with RECCAP regional chapter analyses.

| Region | DGVM mean NBP (TgC $yr^{-1}$) | Region processed-based models | Inventory-based | Flux-based | Inversion | Best estimate |
|---|---|---|---|---|---|---|
| Russia | $-199$ | | $-761$ | $-709$ | $-653$ | |
| South America (forest) | $-472 \pm 211$ | | $-570 \pm 170$ (1990–94)<br>$-530 \pm 140$ (1995–99)<br>$-450 \pm 250$ (2000–04)<br>$-150 \pm 230$ (2005–09) | | | |
| Africa | $-410 \pm 310$ | | $-740 \pm 1190$ | $-1340 \pm 1320$ | $50 \pm 280$<br>(LULCC $510 \pm 280$) | |
| Australia & New Zealand | $-70 \pm 78$ | $-36 \pm 29$<br>(LULCC $18 \pm 7$) | | | | |
| Europe | $-179 \pm 92$ | | | | | $-891 \pm 155$<br>(2001–05) |
| Arctic (1990–2006) | $-86$ | $-177$ | | | | $-96$ |
| South Asia | $-210 \pm 164$ | | | | $-35.4$ (1997–06)<br>$-317$ to $-88.3$ (2007–08) | |
| East Asia | $-224 \pm 141$ | | $-293 \pm 33$ combined inventory–EO-flux approach | | | $270 \pm 507$ |

"natural" decadal-scale variability; however, largely based on the results of McKinley et al. (2011) and Fay and McKinley (2013), who showed that whereas trends in oceanic $pCO_2$ (and air–sea $CO_2$ fluxes) are variable on a decadal timescale, they do converge towards atmospheric $pCO_2$ trends when analysed over a longer 30-year period for most global regions. Nevertheless, they also show that warming (partly driven by anthropogenic climate change) in the permanently stratified subtropical gyre of the North Atlantic has started to reduce ocean uptake in recent years. In the Southern Ocean, where Le Quéré et al. (2007) and Lovenduski et al. (2008) used models to suggest a reduction in ocean carbon uptake efficiency over the past 25 years in response to increasing Southern Ocean winds, Fay and McKinley (2013) concluded that the data are insufficient to draw any conclusions.

We should note that the associated uncertainties remain large. Of particular concern is the moderate success of the models in simulating the time-mean ocean sinks and their long-term seasonal cycle (e.g. McKinley et al., 2006). Furthermore, some of the models underestimate the oceanic uptake of transient tracers such as anthropogenic radiocarbon (see e.g. Graven et al., 2012). Such a reduction in the oceanic uptake efficiency is also not suggested by independent measures of oceanic $CO_2$ uptake, such as the atmospheric $O_2$ / $N_2$ method (Manning and Keeling, 2006; Ishidoya et al., 2012), although the large uncertainties in these estimates make the determination of trends in uptake highly uncertain.

All the models have been tuned to reproduce data synthesis on ocean surface $pCO_2$ (Pfeil et al., 2013; Takahashi et al., 2009) and deep ocean (Key et al., 2004) reasonably well. Specific systematic data assimilation procedures, however, have not been applied. On decadal timescales, the ocean $CO_2$ flux feedback to climate change (change in hydrography and circulation) and rising ambient $CO_2$ (change in $CO_2$ buffering) reacts only slowly on the global average due to the long timescales of oceanic motion and marine $CO_2$ equilibration with the atmosphere. Changes in biogeochemical and ecosystem processes, such as locally varying gas exchange velocities, phytoplankton blooms, and associated particle flux pulses, can lead to regional interannual variations in air–sea $CO_2$ fluxes, but may partially cancel for averages over larger regions. With ocean observations only over about a two-decade time frame, it is difficult to quantify longer-term trends due to other proposed mechanisms: a gradual slowing-down of meridional overturning circulation due to a strengthening of density stratification; redissolution of $CaCO_3$ sediment from the seafloor associated with fossil fuel neutralization; and potential changes in biogenic particle fluxes due to carbon overconsumption and changing ballasting (cf. Keller et al., 2014). Whether more complex models will render better results will depend on how well the additional free parameters in more complex biogeochemical models can be constrained by measurements. So far, more complex – and hence potentially more realistic – models do not necessarily give better results than the present nutrient-phytoplankton-zooplankton-detritus (NPZD)-type models models as applied here (Le Quéré et al., 2005; Kriest et al., 2010).

### 4.3 Reducing uncertainty in regional sinks

In order to better quantify the regional carbon cycle and its trends, DGVM and ocean carbon cycle models need to improve both process representations and model evaluation and benchmarking (Luo et al., 2012). There is a need for up-to-date global climate and land use and cover change data sets to force the DGVMs, as well as a deeper investigation of the quality and differences between the different reanalysis products used to force ocean carbon cycle models. Also, techniques such as detection and attribution can be applied to elucidate trends in the regional carbon cycle and their drivers.

#### 4.3.1 Model evaluation and benchmarking

Piao et al. (2013) evaluated the DGVM model results for their response to climate variability and to $CO_2$ trends, and the seasonal cycle of $CO_2$ fluxes were benchmarked in Peng et al. (2014). Piao et al. (2013) found DGVMs to simulate higher mean and interannual variations (IAVs) in gross primary production than a data-driven model (Jung et al., 2011), particularly in the tropics; however, this is the region where the data-driven model is most uncertain. DGVMs were able to capture the IAVs in RLS, although the simulated land–atmosphere net $CO_2$ flux appears too sensitive to variations in precipitation in tropical forests and savannas. However, Poulter et al. (2014) found an increase in the sensitivity of the net flux to precipitation over the last three decades across continental Australia. Piao et al. (2013) found that the simulated net $CO_2$ flux was more sensitive than productivity to temperature variations. When compared to ecosystem warming experiments the DGVMs tend to underpredict the response of NPP to temperature at temperate sites. DGVMs simulated an ensemble mean NPP enhancement comparable to FACE experiment observations (Piao et al., 2013). However, modelling of ecosystem function in water-stressed environments and changes in plant water use with elevated $CO_2$ remains a challenge for DGVMs (Morales et al., 2005; Keenan et al., 2009; De Kauwe et al., 2013).

There is a critical need for comprehensive model benchmarking, as a first step to attempt to reduce model uncertainty. Several prototype carbon cycle benchmarking schemes have been developed (Randerson et al., 2009; Cadule et al., 2010). A more in-depth evaluation and community benchmarking set needs to be agreed upon and implemented which also evaluates models for their implicit land response timescales (especially relevant in the discussion on future tipping elements and non-linear future responses) and for the simulated carbon, water, and nutrient cycles. New emerging frameworks now exist (Blyth et al., 2011; Abramowitz, 2012; Luo et al., 2012; Dalmonech and Zaehle, 2013; Harverd et al., 2013). One example within RECAPP is a multiple-constraint approach applied to reduce uncertainty in land carbon and water cycles over Australia (Haverd et al., 2013).

#### 4.3.2 Model resolution

Simulated ocean carbon dynamics may be sensitive to horizontal resolution, particularly as model resolution improves sufficiently to adequately capture mesoscale eddies. Mesoscale turbulence influences the ocean carbon cycle in a variety of ways, and the present eddy parameterisations may not adequately capture the full range of effects and the responses to climate variability and change. For example, mesoscale processes are thought to modulate biological productivity by altering the supply of limiting nutrients (Falkowski et al., 1991; McGillicuddy et al., 1998; Gruber et al., 2011). A particularly crucial issue involves the wind-driven overturning circulation in the Southern Ocean, where non-eddy-resolving models indicate a strong sensitivity of the overturning circulation and ocean carbon uptake to surface wind stress (Le Quéré et al., 2007; Lovenduski et al., 2008). Some eddy-resolving models, in contrast, suggest that enhanced wind stress is dissipated by increased eddy activity, leading to only a small increase in overturning (Böning, et al., 2008), although more recent results indicate a larger response (Gent and Danabasoglu, 2011; Matear et al., 2013).

#### 4.3.3 Model structure

There is a need for improved representation of ecological processes in land and ocean models, e.g. nutrient cycling (N, P), demographic dynamics, disturbance (wildfire, windthrow, insects), land use and land cover change in land models, and better representation of the key functional diversity in ocean and land biogeochemical models. DGVMs need to represent land use and land cover changes, forest management, and forest age in order to improve estimates of the regional and global land carbon budget. There have been recent developments to include nutrient dynamics, mostly nitrogen, in global land biosphere models (as reviewed by Zaehle and Dalmonech, 2011). Too few model simulations are available to date to allow for an ensemble model trend assessment. However, a few general trends appear robust: as evident from Table 3, CN models generally show less of a response to increasing atmospheric $CO_2$ due to nitrogen limitation of plant production. N dynamics further alter the climate–carbon relationship, which tend to reduce the C loss from temperate and boreal terrestrial ecosystems due to warming – but with a considerable degree of uncertainty (Thornton et al., 2009; Sokolov et al., 2008; Zaehle et al., 2010). Changes in the nitrogen cycle due to anthropogenic reactive nitrogen additions (both fertiliser to croplands and N deposition on forests and natural grasslands) further modify the terrestrial net C balance and contribute with $-0.2$ to $-0.5\,\mathrm{Pg\,C\,yr^{-1}}$ to the current land sink (Zaehle and Dalmonech, 2011). Zaehle et al. (2011), using the OCN model, estimated the 1995–2005 trend in land uptake due to N deposition to be $-1.1 \pm 1.7\,\mathrm{Tg\,C\,yr^{-2}}$, with strong regional differences depending on the regional trends in air pollution and reactive N loading of the atmosphere and the nitrogen status of the ecosystems, which are generally lower in less responsive ecosystems close to nitrogen saturation highly polluted regions. The DGVMs applied here do not consider the P cycle; P limitation on land carbon uptake may be particularly important in tropical forests and savannas (Edwards et al., 2005; Wang et al., 2010; Zhang et al., 2014).

There are several additional land processes that have not been considered in this current multi-model analysis. These include the effects of aerosols and tropospheric ozone on the carbon cycle. Unlike a global forcing agent such as $CO_2$, the effects of air pollutants (aerosols, $NO_x$, and $O_3$), with their shorter atmospheric lifetimes, are at the regional scale.

Aerosol-induced changes in radiation quantity and quality (i.e. the ratio of diffuse to direct) affect plant productivity and the land sink (Mercado et al., 2009). From around 1960 until the 1980s, radiation levels declined across industrialised regions, a phenomenon called "global dimming", followed by a recent brightening in Europe and North America with the adoption of air pollution legislation. Reductions in acid rain have been found to greatly influence trends in riverine DOC, vegetation health, and rates of soil organic matter decomposition. Tropospheric ozone is known to be toxic to plants and lead to reductions in plant productivity, and thus reduce the efficiency of the land carbon sink (Sitch et al., 2007b; Anav et al., 2011). Drivers of the land carbon sink related to air pollution – e.g. N deposition, acid precipitation, diffuse and direct radiation, and surface $O_3$ – have varied markedly in space and time over recent decades. Although likely important for regional carbon cycle trends, quantifying these effects is beyond the scope of the present study.

The Pinatubo eruption in 1991, at the start of the study period, had a major influence on many carbon cycle processes, leading to an enhanced land sink over the period 1991–1993. This has been attributed to a combination of cooling-induced reductions in high-latitude respiration and enhanced productivity associated with changes in diffuse radiation (Jones and Cox, 2001; Lucht et al., 2002; Peylin et al., 2005; Mercado et al., 2009; Frölicher et al., 2013). The direct effect of aerosols on climate drivers is implicitly included in this study (i.e. responses to high-latitude cooling, tropical drying, reduced net incoming solar radiation); however diffuse radiation effects are not included.

Similar gaps need to be addressed in ocean biogeochemical models. The ecosystem modules in the current generation of OBGCMs lack the ability to assess many of the suggested mechanisms by which climate and ocean acidification could alter marine biogeochemistry and ocean carbon storage. Proposed biological processes that could influence ocean carbon uptake and release involve, for example, decoupling of carbon and macronutrient cycling, changes in micronutrient limitation, variations in elemental stoichiometry in organic matter, and changes in the vertical depth scale for the respiration of sinking organic carbon particles (e.g. Boyd and Doney, 2003; Sarmiento and Gruber, 2006). Some advances have been made with the incorporation of dynamic iron cycling and iron limitation, multiple plankton groups, calcification, and nitrogen fixation (Le Quéré et al., 2005). However, the evaluation of these aspects of the models is currently hindered by both data- and process-level information limitations.

#### 4.3.4 Climate and land use and cover data sets

In addition to model structure, the choice of climate forcing and model initial conditions can also contribute to differences in the simulated terrestrial carbon sink. At regional scales, differences in land cover can introduce $\sim 10\,\%$ uncertainty in simulated regional-scale GPP (Jung et al., 2007; Quaife et al., 2008) and $\sim 3.5\,\%$ uncertainty for global NPP. Climate forcing uncertainty tends to have larger effects on carbon flux uncertainty than land cover (Hicke, 2005; Poulter et al., 2011), with up to 25 % differences in GPP reported over Europe (Jung et al., 2007) and a 10 % difference for global NPP (Poulter et al., 2011). Climate forcing uncertainty and land cover (i.e. PFT distributions) can alter long-term trends in land to atmosphere net $CO_2$ flux and interannual variability of carbon fluxes to climate (Poulter et al., 2011). The DGVMs applied here did not consider LULCC. This is an active area of research; models need a consistent implementation of LULCC. Uncertainties in the simulated net land use flux are associated with assumptions on the implementation of LULCC gridded maps (e.g. whether conversion to cropland in a grid-cell is taken preferentially from grassland, forest, or both), simulated biomass estimates, and subsequent decomposition rates. However DGVMs offer the exciting prospect of disentangling the component fluxes associated with land use (e.g. direct emissions and legacy fluxes) and separating the environmental and direct human impacts on the net LU flux (Gasser and Ciais, 2013; Pongratz et al., 2014; Stocker et al., 2014).

## 5 Conclusions

Land models suggest an increase in the global land net C uptake over the period 1990–2009, with increases in tropical and southern regions and negligible increase in northern regions. The increased sink is mainly driven by trends in NPP, in response to increasing atmospheric $CO_2$ concentration, and modulated by change in climate. Over the same period, ocean models suggest a negligible increase in net ocean C uptake – a result of ocean warming counteracting the expected increase in ocean uptake driven by the increase in atmospheric $CO_2$. At the sub-regional level, trends vary both in sign and magnitude, particularly over land. Areas in temperate North America, eastern Europe, and northeastern China show a decreasing regional land sink trend, due to regional drying, suggesting a possibility for a transition to a net carbon source in the future if drying continues or droughts become more severe and/or frequent. In the ocean, the trends tend to be more homogeneous, but the underlying dynamics differ greatly, ranging from ocean warming, to winds, and to changes in circulation/mixing and ocean productivity, making simple extrapolations into the future difficult.

Our conclusions need to be viewed with several important caveats: only a few models include a fully coupled carbon–nitrogen cycle, and no model included land use and land cover changes. Ocean models tend to be too coarse in resolution to properly represent important scales of motions and mixing, such as eddies and other mesoscale processes, and coastal boundary processes. Furthermore, their representation of ocean ecosystem processes and their sensitivity to

climate change and other stressors (e.g. ocean acidification, deoxygenation, etc.; Gruber, 2011; Boyd, 2011) is rather simplistic.

There is a need for detailed model evaluation and benchmarking in order to reduce the uncertainty in the sinks in the land and ocean and, particularly, in how these sinks have changed in the past and how they may change in the future. For land ecosystems, a concerted effort is needed in the DGVM community to incorporate nutrient cycling as well as land use and land cover change. For the oceans, models need to improve their representation of unresolved physical transport and mixing processes, and ecosystem models need to evolve to better characterise their response to global change.

**The Supplement related to this article is available online at doi:10.5194/bg-12-653-2015-supplement.**

*Acknowledgements.* S. Sitch acknowledges financial support by RCUK through NERC (grant no. NE/J010154/). N. Gruber and C. Heinze acknowledge financial support by the European Commission through the EU FP7 projects CARBOCHANGE (grant no. 264879) and GEOCARBON (grant no. 283080). N. Gruber was additionally supported through ETH Zurich. S. C. Doney acknowledges support from the US National Science Foundation (NSF AGS-1048827). P. Friedlingstein, A. Arneth, and S. Zaehle acknowledge support by the European Commission through the EU FP7 project EMBRACE (grant no. 282672). A. Arneth and S. Sitch acknowledge the support of the European Commission-funded project LUC4C (grant no. 603542). The research leading to these results received funding from the European Community's Seventh Framework Programme (FP7 2007–2013) under grant agreement no. 238366. A. Ahlström and B. Smith acknowledge funding through the Mistra Swedish Research Programme on Climate, Impacts and Adaptation (SWECIA). This study is a contribution to the Lund Centre for Studies of Carbon Cycle and Climate Interactions (LUCCI) and the Strategic Research Area Modelling the Regional and Global Earth System (MERGE). This is a contribution to the Bjerknes Centre for Climate Research (BCCR) and core project BIOFEEDBACK of the Centre for Climate Dynamics (SKD) at BCCR. C. Heinze acknowledges support from NOTUR/NorStore projects NN2980K and NS2980K. The authors wish to thank Jonathan Barichivich for discussions on greening trends.

Edited by: F. Joos

## References

Abramowitz, G.: Towards a public, standardized, diagnostic benchmarking system for land surface models, Geosci. Model Dev., 5, 819–827, doi:10.5194/gmd-5-819-2012, 2012.

Allen, C. D., Macalady, A., Chenchouni, H., Bachelet, D., McDowell, N., Vennetier, M., Gonzales, P., Hogg, T., Rigling, A., Breshears, D., Fensham, R., Zhang, Z., Kitzberger, T., Lim, J., Castro, J., Allard, G., Running, S., Semerci, A., and Cobb, N.: A global overview of drought and heat-induced tree mortality reveals emerging climate change risks for forests, Forest Ecol. Manag., 4, 660–684, doi:10.1016/j.foreco.2009.09.001, 2010.

Anav, A., Menut, L., Khvorostyanov, D., and Viovy, N.: Impact of tropospheric ozone on the Euro-Mediterranean vegetation, Glob. Change Biol., 17, 2342–2359, 2011.

Anderegg, W. R. L., Berry J. A., Smith, D. D., Sperry J. S., Anderegg, L. D. L., and Field, C. B.: The roles of hydraulic and carbon stress in a widespread climate-induced forest die-off, P. Natl. Acad. Sci. USA, 109, 233–237, doi:10.1073/pnas.1107891109, 2012.

Angert, A., Biraud, S., Bonfils, C., Henning, C. C., Buermann, W., Pinzon, J., Tucker, C. J., and I. Fung: Drier summers cancel out the $CO_2$ uptake enhancement induced by warmer springs, P. Natl. Acad. Sci., 102, 10823–10827, 2005.

Assmann, K. M., Bentsen, M., Segschneider, J., and Heinze, C.: An isopycnic ocean carbon cycle model, Geosci. Model Dev., 3, 143–167, doi:10.5194/gmd-3-143-2010, 2010.

Baker, T. R., Phillips, O. L., Malhi, Y., Almeida, S., Arroyo, L., Di Fiore, A., Erwin, T., Higuchi, N., Killeen, T. J., Laurance, S. G., Laurance, W. F., Lewis, S. L., Monteagudo, A., Neill, D. A., Nunez Vargas, P., Pitman, N. C. A., Silva, J. N. M., and Vasquez Martinez, R.: Increasing biomass in Amazonian forest plots, Philos. T. R. Soc. B, 359, 353–365, 2004.

Ballantyne, A. P., Alden, C. B., Miller, J. B., Tans, P. P., and White, J. W. C.: Increase in observed net carbon dioxide uptake by land and oceans during the past 50 years, Nature, 488, 70–72, doi:10.1038/nature11299, 2012.

Beck, S. A. and Goetz, S. J.: Satellite observations of high northern latitude vegetation productivity changes between 1982 and 2008: ecological variability and regional differences, Environ. Res. Lett. 6, 045501, doi:10.1088/1748-9326/6/4/045501, 2011.

Bhatt, U. S., Walker, D. A., Raynolds, M. K., Comiso, J. C., Epstein, H. E., Jia, G., Gens, R., Pinzon, J. E., Tucker, C. J., Tweedie, C. E., and Webber, P. J.: Circumpolar Arctic tundra vegetation change is linked to sea ice decline, Earth Interact., 14, 1–20, 2010.

Blyth, E., Clark, D. B., Ellis, R., Huntingford, C., Los, S., Pryor, M., Best, M., and Sitch, S.: A comprehensive set of benchmark tests for a land surface model of simultaneous fluxes of water and carbon at both the global and seasonal scale, Geosci. Model Dev., 4, 255–269, doi:10.5194/gmd-4-255-2011, 2011.

Bonan, G. B. and Levis, S.: Quantifying carbon-nitrogen feedbacks in the Community Land Model (CLM4), Geophys. Res. Lett., 37, L07401, doi:10.1029/2010GL042430, 2010.

Bond-Lamberty, B., Peckham, S. D., Ahl, D. E., and Gower, S. T.: Fire as the dominant driver of central Canadian boreal forest carbon balance, Nature, 450, 89–92, 2007.

Böning, C. W., Dispert, A., Visbeck, M., Rintoul, S. R., and Schwarzkopf, F. U.: The response of the Antarctic Circumpolar Current to recent climate change, Nat. Geosci., 1, 864–869, 2008.

Boyd, P. and Doney, S. C.: The impact of climate change and feedback process on the ocean carbon cycle, Ocean Biogeochemistry, edited by: Fasham, M., Springer, 157–193, 2003.

Boyd, P. W.: Beyond ocean acidification, Nat. Geosci., 4, 273–274, 2011.

Broecker, W. S., Peng, T.-H., Ostlund, G., and Stuiver, M.: The distribution of bomb radiocarbon in the ocean, J. Geophys. Res., 90, 6953–6970, 1985.

Buermann, W., Lintner, B. R., Koven, C. D., Angert, A., Pinzon, J. E., Tucker, C. J., and Fung, I. Y.: The changing carbon cycle at Mauna Loa observatory, P. Natl. Acad. Sci., 104, 4249–4254, 2007.

Buitenhuis, E. T., Rivkin, R. B., Sailley, S., and Le Quéré, C.: Biogeochemical flues through microzooplankton, Global Biogeochem. Cy., 24, GB4015, doi:10.1029/2009GB003601, 2010.

Cadule, P., Friedlingstein, P., Bopp, L., Sitch, S., Jones, C. D., Ciais, P., Piao, S. L., and Peylin, P.: Benchmarking coupled climate-carbon models against long-term atmospheric $CO_2$ measurements, Global Biogeochem. Cy., 24, Gb2016, doi:10.1029/2009gb003556, 2010.

Canadell, J. G., Pataki D., Gifford, R., Houghton, R. A., Lou, Y., Raupach, M. R., Smith, P., and Steffen, W.: Saturation of the terrestrial carbon sink, in: Terrestrial Ecosystems in a Changing World, edited by: Canadell, J. G., Pataki, D., and Pitelka, L., 59–78, The IGBP Series, Springer-Verlag, Berlin Heidelberg, 59–78, 2007.

Canadell, J. G., Ciais, P., Gurney, K., Le Quéré, C., Piao, S., Raupach, M. R., and Sabine, C. L.: An international effort to quantify regional carbon fluxes, EOS T. Am. Geophys. Un., 92, 81–82, 2011.

Canadell, J. G., Ciais, P., Sabine, C., and Joos, F. (Eds.): REgional Carbon Cycle Assessment and Processes (RECCAP), Special issue, Biogeosciences, http://www.biogeosciences-discuss.net/special_issue83.html, 2013.

Chevallier, F., Ciais, P., Conway, T. J., Aalto, T., Anderson, B. E., Bousquet, P., Brunke, E. G., Ciattaglia, L., Esaki, Y., Fröhlich, M., Gomez, A., Gomez-Pelaez, A. J., Haszpra, L., Krummel, P. B., Langenfelds, R. L., Leuenberger, M., Machida, T., Maignan, F., Matsueda, H., Morguí, J. A., Mukai, H., Nakazawa, T., Peylin, P., Ramonet, M., Rivier, L., Sawa, Y., Schmidt, M., Steele, L. P., Vay, S. A., Vermeulen, A. T., Wofsy, S., and Worthy, D.: $CO_2$ surface fluxes at grid point scale estimated from a global 21-year reanalysis of atmospheric measurements, J. Geophys. Res., 115, D21307, doi:10.1029/2010JD013887, 2010.

Ciais, P., Tans, P. P., Trolier, M., White, J. W. C., and Francey, R. J.: A large northern hemisphere terrestrial $CO_2$ sink indicated by the $^{13}C / ^{12}C$ ratio of atmospheric $CO_2$, Science, 269, 1098–1102, doi:10.1126/science.269.5227.1098, 1995.

Ciais, P., Reichstein, M., Viovy, N., Granier, A., Ogee, J., Allard, V., Aubinet, M., Buchmann, N., Bernhofer, C., Carrara, A., Chevallier, F., De Noblet, N., Friend, A. D., Friedlingstein, P., Grunwald, T., Heinesch, B., Keronen, P., Knohl, A., Krinner, G., Loustau, D., Manca, G., Matteucci, G., Miglietta, F., Ourcival, J. M., Papale, D., Pilegaard, K., Rambal, S., Seufert, G., Soussana, J. F., Sanz, M. J., Schulze, E. D., Vesala, T., and Valentini, R.: Europe-wide reduction in primary productivity caused by the heat and drought in 2003, Nature, 437, 529–533, doi:10.1038/nature03972, 2005.

Ciais, P., Canadell, J. G, Luyssaert, S., Chevallier, F., Shvidenko, A., Pousii, Z., Jonas, M., Peylin, P., Wayne King, A., Schulze, E.-D., Piao, S., Roedenbeck, C., Wouters, P., and Breon, F.-M.: Can we reconcile atmospheric estimates of the Northern terrestrial carbon sink with land-based accounting?, Current Opinion in Environmental Sustainability, 2, 225–230, 2010.

Ciais, P., Sabine, C., Bala, G., Bopp, L., Brovkin, V., Canadell, J., Chhabra, A., DeFries, R., Galloway, J., Heimann, M., Jones, C., Le Quéré, C., Myneni, R. B., Piao, S., and Thornton, P.: Carbon and Other Biogeochemical Cycles, in: Climate Change 2013: The Physical Science Basis, Contribution of Working Group I to the Fifth Assessment Report of the Intergovernmental Panel on Climate Change, edited by: Stocker, T. F., Qin, D., Plattner, G.-K., Tignor, M., Allen, S. K., Boschung, J., Nauels, A., Xia, Y., Bex, V., and Midgley, P. M., Cambridge University Press, Cambridge, United Kingdom and New York, NY, USA, 465–570, 2013.

Clark, D. B., Mercado, L. M., Sitch, S., Jones, C. D., Gedney, N., Best, M. J., Pryor, M., Rooney, G. G., Essery, R. L. H., Blyth, E., Boucher, O., Harding, R. J., Huntingford, C., and Cox, P. M.: The Joint UK Land Environment Simulator (JULES), model description – Part 2: Carbon fluxes and vegetation dynamics, Geosci. Model Dev., 4, 701–722, doi:10.5194/gmd-4-701-2011, 2011.

Cox, P. M.: Description of the "TRIFFID" dynamic global vegetation model, Hadley Centre Technical Note, 24, 1–16, 2001.

Dalmonech, D. and Zaehle, S.: Towards a more objective evaluation of modelled land-carbon trends using atmospheric $CO_2$ and satellite-based vegetation activity observations, Biogeosciences, 10, 4189–4210, doi:10.5194/bg-10-4189-2013, 2013.

De Kauwe, M. G., Medlyn, B. E., Zaehle, S., Walker, A. P., Dietze, M. C., Hickler, T., Jain, A. K., Luo, Y., Parton, W. J., Prentice, C., Smith, B., Thornton, P. E., Wang, S., Wang, Y-P., Wårlind, D., Weng, E. S., Crous, K, Y., Ellsworth, D. S., Hanson, P. J., Seok-Kim, H., Warren, J. M., Oren, R., and Norby, R. J.: Forest water use and water use efficiency at elevated $CO_2$: a model-data intercomparison at two contrasting temperate forest FACE sites, Glob. Change Biol., 19, 1759–1779, 2013.

Denman, K. L., Brasseur, G., Chidthaisong, A., Ciais, P., Cox, P. M., Dickinson, R. E., Hauglustaine, D., Heinze, C., Holland, E., Jacob, D., Lohmann, U., Ramachandran, S., da Silva Dias, P. L., Wofsy, S. C. , and Zhang, X.: Couplings Between Changes in the Climate System and Biogeochemistry, in: Climate Change 2007: The Physical Science Basis, Contribution of Working Group I to the Fourth Assessment Report of the Intergovernmental Panel on Climate Change, edited by: Solomon, S., Qin, D., Manning, M., Chen, Z., Marquis, M., Averyt, K. B., Tignor, M., and Miller, H. L., Cambridge University Press, Cambridge, United Kingdom and New York, NY, USA, 499–588, 2007.

Dentener, F., Stevenson, D., Ellingsen, K., van Noije, T., Schultz, M., Amann, M., Atherton, C., Bell, N., Bergmann, D., Bey, I., Bouwman, L., Butler, T., Cofala, J., Collins, B., Drevet, J., Doherty, R., Eickhout, B., Eskes, H., Fiore, A., Gauss, M., Hauglustaine, D., Horowitz, L., Isaksen, I. S. A., Josse, B., Lawrence, M., Krol, M., Lamarque, J. F., Montanaro, V., Muller, J. F., Peuch, V. H., Pitari, G., Pyle, J., Rast, S., Rodriguez, J., Sanderson, M., Savage, N. H., Shindell, D., Strahan, S., Szopa, S., Sudo, K., Van Dingenen, R., Wild, O., and Zeng, G.: The global atmospheric environment for the next generation, Environ. Sci. Technol., 40, 3586–3594, doi:10.1021/es0523845, 2006.

Dolman, A. J., Shvidenko, A., Schepaschenko, D., Ciais, P., Tchebakova, N., Chen, T., van der Molen, M. K., Belelli Marchesini, L., Maximov, T. C., Maksyutov, S., and Schulze, E.-D.: An estimate of the terrestrial carbon budget of Russia using inventory-based, eddy covariance and inversion methods, Biogeosciences, 9, 5323–5340, doi:10.5194/bg-9-5323-2012, 2012.

Doney, S. C., Lima, I., Feely, R. A., Glover, D. M., Lindsay, K., Mahowald, N., Moore, J. K., and Wanninkhof, R.: Mechanisms governing interannual variability in upper-ocean inorganic carbon system and air-sea $CO_2$ fluxes: Physical climate and atmospheric dust, Deep-Sea Res.-Pt. II, 56, 640–655, 2009a.

Doney, S. C., Lima, I., Moore, J. K., Lindsay, K., Behrenfeld, M. J., Westberry, T. K., Mahowald, N., Glover, D. M., and Takahashi, T.: Skill metrics for confronting global upper ocean ecosystem-biogeochemistry models against field and remote sensing data, J. Marine Syst., 76, 95–112, doi:10.1016/j.jmarsys.2008.05.015, 2009b.

Edwards E., S. McCaffery, S., and Evans, J.: Phosphorus status determines biomass response to elevated $CO_2$ in a legume: C-4 grass community, Glob. Change Biol., 11, 1968–1981, 2005.

Falkowski, P. G., Ziemann, D., Kolber, Z., and Bienfang, P. K.: Role of eddy pumping in enhancing primary production in the ocean, Nature, 352, 55–58, 1991.

Fan, S., Gloor, M., Mahlmam, J., Pacala, S., Sarmiento, J., Takahashi, T., and Tans, P.: A large terrestrial carbon sink in North America implied by atmospheric and oceanic carbon dioxide data and models, Science, 282, 442–446, 1998.

Fay, A. R. and McKinley, G. A.: Global trends in surface ocean $p$CO2 from in situ data, Global Biogeochem. Cy., 27, 541–557, doi:10.1002/gbc.20051, 2013.

Friedlingstein, P., Houghton, R. A., Marland, G., Hackler, J., Boden,T. A., Conway, T. J., Canadell, J. G., Raupach, M. R., Ciais, P., and Le Quéré, C.: Update on $CO_2$ emissions, Nat. Geosci., 3, 811–812, doi:10.1038/ngeo1022, 2010.

Friend, A. D., Stevens, A. K., Knox, R. G., and Cannell, M. G. R.: A process-based, terrestrial biosphere model of ecosystem dynamics (Hybrid v3.0), Ecol. Model., 95, 249–287, 1997.

Frölicher, T. L., Joos, F., Raible, C. C., and Sarmiento, J. L.: Atmospheric $CO_2$ response to volcanic eruptions: the role of ENSO, season, and variability, Global Biogeochem. Cy., 27, 239–251, 2013.

Gasser, T. and Ciais, P.: A theoretical framework for the net land-to-atmosphere $CO_2$ flux and its implications in the definition of "emissions from land-use change", Earth Syst. Dynam., 4, 171–186, doi:10.5194/esd-4-171-2013, 2013.

Gent, P. R. and Danabasoglu, G.: Response to Increasing Southern Hemisphere Winds in CCSM4, J. Climate, 24, 4992–4998, 2011.

Gloor, M., Gruber, N., Sarmiento, J. L., Sabine, C., Feely, D., and Rödenbeck, C.: A first estimate of present and preindustrial air-sea $CO_2$ flux patterns based on ocean interior carbon measurements and models, Geophys. Res. Lett., 30, 1010, doi:10.1029/2002GL015594, 2003.

Gloor, M., Sarmiento, J. L., and Gruber, N.: What can be learned about carbon cycle climate feedbacks from the $CO_2$ airborne fraction?, Atmos. Chem. Phys., 10, 7739–7751, doi:10.5194/acp-10-7739-2010, 2010.

Gloor, M., Gatti, L., Brienen, R., Feldpausch, T. R., Phillips, O. L., Miller, J., Ometto, J. P., Rocha, H., Baker, T., de Jong, B., Houghton, R. A., Malhi, Y., Aragão, L. E. O. C., Guyot, J.-L., Zhao, K., Jackson, R., Peylin, P., Sitch, S., Poulter, B., Lomas, M., Zaehle, S., Huntingford, C., Levy, P., and Lloyd, J.: The carbon balance of South America: a review of the status, decadal trends and main determinants, Biogeosciences, 9, 5407–5430, doi:10.5194/bg-9-5407-2012, 2012.

Graven, H. D., Gruber, N., Key, R., Khatiwala, S., and Giraud, X.: Changing controls on oceanic radiocarbon: New insights on shallow-to-deep ocean exchange and anthropogenic $CO_2$ uptake, J. Geophys. Res., 117, C10005, doi:10.1029/2012JC008074, 2012.

Gruber, N.: Warming up, turning sour, losing breath: Ocean biogeochemistry under global change, Philos. T. R. Soc. A, 369, 1980–1996, doi:10.1098/rsta.2011.0003, 2011.

Gruber, N., Gloor, M., Fletcher, S. E. M., Doney, S. C., Dutkiewicz, S., Follows, M. J., Gerber, M., Jacobson, A. R., Joos, F., Lindsay, K., Menemenlis, D., Mouchet, A., Muller, S. A., Sarmiento, J. L., and Takahashi, T.: Oceanic sources, sinks, and transport of atmospheric $CO_2$, Global Biogeochem. Cy., 23, GB1005, doi:10.1029/2008GB003349, 2009.

Gruber, N., Lachkar, Z., Frenzel, H., Marchesiello, P., Munnich, M., McWilliams, J., Nagai, T., and Plattner, G.-K.: Eddy-induced reduction of biological production in Eastern Boundary Upwelling Systems, Nat. Geosci., 4, 787–792, doi:10.1038/ngeo1273, 2011.

Haverd, V., Raupach, M. R., Briggs, P. R., J. G. Canadell., Davis, S. J., Law, R. M., Meyer, C. P., Peters, G. P., Pickett-Heaps, C., and Sherman, B.: The Australian terrestrial carbon budget, Biogeosciences, 10, 851–869, doi:10.5194/bg-10-851-2013, 2013.

Hicke, J. A.: NCEP and GISS solar radiation data sets available for ecosystem modeling: Description, differences, and impacts on net primary production, Global Biogeochem. Cy., 19, GB2006, doi:10.1029/2004GB002391, 2005.

Houghton, R. A.: How well do we know the flux of $CO_2$ from land-use change? Tellus B, 62, 337–351, doi:10.1111/j.1600-0889.2010.00473.x, 2010.

Ishidoya, S., Aoki, S., Goto, D., Nakazawa, T., Taguchi, S., and Patra, P. K.: Time and Space variations of $O_2/N_2$ ratio in the troposphere over Japan and estimation of the global $CO_2$ budget for the period 2000–2010, Tellus B, 64, 18964, doi:10.3402/tellusb.v64i0.18964, 2012.

Janssens, I. A., Freibauer, A., Ciais, P., Smith, P., Nabuurs, G.-J., Folberth, G., Schlamadinger, B., Hutjes, R. W. A., Ceulemans, R., Schulze, E.-D., Valentini, R., and Dolman, A. J.: Europe's terrestrial biosphere absorbs 7 to 12 % of European anthropogenic $CO_2$ emissions, Science 300, 1538–1542, 2003.

Jones, C. D. and Cox, P. M.: Modelling the volcanic signal in the atmospheric $CO_2$ record, Global Biogeochem. Cy., 15, 453–465, doi:10.1029/2000GB001281, 2001.

Jönsson, A. M., Schröder, M., Lagergren, F., Anderbrandt, O., and Smith, B.: Guess the impact of *Ips typographus* – an ecosystem modelling approach for simulating bark beetle outbreaks, Agr. Forest Meteorol., 166–167, 188–200, 2012.

Jung, M., Vetter, M., Herold, M., Churkina, G., Reichstein, M., Zaehle, S., Cias, P., Viovy, N., Bondeau, A., Chen, Y., Trusilova, K., Feser, F., and Heimann, M.: Uncertainties of modelling GPP over Europe: A systematic study on the effects of using different drivers and terrestrial biosphere models, Global Biogeochem. Cy., 21, GB4021, doi:10.1029/2006GB002915, 2007.

Jung, M., Reichstein, M., Margolis, H. A., Cescatti, A., Richardson A. D., Arain, M. A., Arneth, A., Bernhofer, C., Bonal, D., Chen J., Gianelle, D., Gobron, N., Kiely, G., Kutsch, W., Lasslop, G., Law, B. E., Lindroth, A., Merbold, L., Montagnani, L., Moors, E. J., Papale, D., Sottocornola, M., Vaccari, F., and Williams, C.: Global patterns of land-atmosphere fluxes of carbon dioxide, latent heat, and sensible heat derived from eddy covariance,

satellite, and meteorological observations, J. Geophys. Res., 116, G00J07, doi:10.1029/2010JG001566, 2011.

Kalnay, E., Kanamitsu, M., Kistler, R., Collins, W., Deaven, D., Gandin, L., Iredell, M., Saha, S., Woollen, J., Zhu, Y., Chelliah, M., Ebisuzaki, W., Higgins, W., Janowiak, J., Mo, K. C., Ropelewski, C., Wang, J., Leetmaa, A., Reynolds, R., Jenne, R., and Joseph, D.: The NCEP/NCAR 40-year reanalysis project, B. Am. Meteorol. Soc., 77, 437–471, 1996.

Keeling, C. D., Bacastow, R. B., Bainbridge, A. E., Ekdahl Jr, C. A., Guenther, P. R., Waterman, L. S., and Chinm J. F. S.: Atmospheric carbon dioxide variations at Mauna Loa observatory, Hawaii, Tellus, 28, 538–551, 1976.

Keeling, C. D., Whorf, T. P., Wahlen, M., and van der Plicht, J.: Interannual extremes in the rate of rise of atmospheric carbon dioxide since 1980, Nature, 375, 666–670, 1995.

Keenan, T., García, R., Friend, A. D., Zaehle, S., Gracia, C., and Sabate, S.: Improved understanding of drought controls on seasonal variation in Mediterranean forest canopy $CO_2$ and water fluxes through combined in situ measurements and ecosystem modelling, Biogeosciences, 6, 1423–1444, doi:10.5194/bg-6-1423-2009, 2009.

Keller, K. M., Joos, F., and Raible, C. C.: Time of emergence of trends in ocean biogeochemistry, Biogeosciences, 11, 3647–3659, doi:10.5194/bg-11-3647-2014, 2014.

Key, R. M., Kozyr, A., Sabine, C. L., Lee, K., Wanninkhof, R., Bullister, J. L., Feely, R. A., Millero, F. J., Mordy, C., and Peng, T.-H.: A global ocean carbon climatology: results from Global Data Analysis Project (GLODAP), Global Biogeochem. Cy., 18, GB4031, doi:10.1029/2004GB002247, 2004.

Khatiwala, S., Primeau, F., and Hall, T.: Reconstruction of the history of anthropogenic $CO_2$ concentrations in the ocean, Nature, 462, 346–349, doi:10.1038/nature08526, 2009.

Khatiwala, S., Tanhua, T., Mikaloff Fletcher, S., Gerber, M., Doney, S. C., Graven, H. D., Gruber, N., McKinley, G. A., Murata, A., Ríos, A. F., and Sabine, C. L.: Global ocean storage of anthropogenic carbon, Biogeosciences, 10, 2169–2191, doi:10.5194/bg-10-2169-2013, 2013.

Kriest, I., Khatiwala, S., and Oschlies, A.: Towards an assessment of simple global marine biogeochemical models of different complexity, Progr. Oceanogr., 86, 337–360, 2010.

Krinner, G., Viovy, N., de Noblet-Ducoudre, N., Ogee, J., Polcher, J., Friedlingstein, P., Ciais, P., Sitch, S., and Prentice, I. C.: A dynamic global vegetation model for studies of the coupled atmosphere-biosphere system, Global Biogeochem. Cy., 19, Gb1015, doi:10.1029/2003gb002199, 2005.

Kurz, W. A., Dymond, C. C., Stinson, G., Rampley, G. J., Neilson, E. T., Carroll, A. L., Ebata, T., and Safranyik, L.: Mountain pine beetle and forest carbon feedback to climate change, Nature, 452, 987–990, doi:10.1038/nature06777, 2008.

Lagergren, F., Jönsson, A. M., Blennow, K., and Smith, B.: Implementing storm damage in a dynamic vegetation model for regional applications in Sweden, Ecol. Model., 247, 71–82, 2012.

Large, W. G. and Yeager, S.: Diurnal to decadal global forcing for ocean and sea-ice models: The data sets and flux climatologies, NCAR Tech. Rep. TN-460 _STR, 105 pp., 2004.

Lawrence, D. M., Oleson, K. W., Flanner, M. G., Thornton, P. E., Swenson, S. C., Lawrence, P. J., Zeng, X., Yang, Z.-L., Levis, S., Sakaguchi, K., Bonan, G. B., and Slater, A. G.: Parameterization improvements and functional and structural advances in version 4 of the Community Land Model, J. Adv. Model. Earth Syst., 3, M03001, doi:10.1029/2011ms000045, 2011.

Lenton, A., Tilbrook, B., Law, R. M., Bakker, D., Doney, S. C., Gruber, N., Ishii, M., Hoppema, M., Lovenduski, N. S., Matear, R. J., McNeil, B. I., Metzl, N., Mikaloff Fletcher, S. E., Monteiro, P. M. S., Rödenbeck, C., Sweeney, C., and Takahashi, T.: Sea-air $CO_2$ fluxes in the Southern Ocean for the period 1990–2009, Biogeosciences, 10, 4037–4054, doi:10.5194/bg-10-4037-2013, 2013.

Le Quéré, C. L., Harrison, S. P., Colin Prentice, I. C., Buitenhuis, E. T., Aumont, O., Bopp, L., Claustre, H., Cotrim Da Cunha, L., Geider, R., Giraud, X., Klaas, C., Kohfeld, K. E., Legendre, L., Manizza, M., Platt, T., Rivkin, R. B., Sathyendranath, S., Uitz, J., Watson, A. J., and Wolf-Gladrow, D.: Ecosystem dynamics based on plankton functional types for global ocean biogeochemistry models, Glob. Change Biol., 11, 2016–2040, doi:10.1111/j.1365-2486.2005.1004.x, 2005.

Le Quéré, C, Rödenbeck, C., Buitenhuis, E. T., Conway, T. J., Langenfelds, R., Gomez, A., Labuschagne, C., Ramonet, M., Nakazawa, T., Metzl, N., and Gillett, N.: Saturation of the Southern ocean $CO_2$ sink due to recent climate change, Science, 316, 1735–1738, doi:10.1126/science.1136188, 2007.

Le Quéré C, Raupach M. R., Canadell, J. G., Marland, G., Bopp, L., Ciais, P., Conway, T. J., Doney, S. C., Feely, R. A., Foster P, Friedlingstein, P., Gurney, K., Houghton, R. A., House, J. I., Huntingford, C., Levy, P. E., Lomas, M. R., Majkut, J., Metzl, N., Ometto, J. P., Peters, G. P., Prentice, I. C., Randerson, J. T., Running, S. W., Sarmiento, J. L., Schuster, U., Sitch, S., Takahashi, T., Viovy, N., van der Werf , G. R., and Woodward, F. I.: Trends in the sources and sinks of carbon dioxide, Nat. Geosci., 2, 831–836, 2009.

Le Quéré, C., Takahashi, T., Buitenhuis, C. E., Rödenbeck, C., and Sutherland, S.: Impact of climate change and variability on the global oceanic sink of $CO_2$, Global Biogeochem. Cy., 24, GB4007, doi:10.1029/2009GB003599, 2010.

Le Quéré, C., Andres, R. J., Boden, T., Conway, T., Houghton, R. A., House, J. I., Marland, G., Peters, G. P., van der Werf, G. R., Ahlström, A., Andrew, R. M., Bopp, L., Canadell, J. G., Ciais, P., Doney, S. C., Enright, C., Friedlingstein, P., Huntingford, C., Jain, A. K., Jourdain, C., Kato, E., Keeling, R. F., Klein Goldewijk, K., Levis, S., Levy, P., Lomas, M., Poulter, B., Raupach, M. R., Schwinger, J., Sitch, S., Stocker, B. D., Viovy, N., Zaehle, S., and Zeng, N.: The global carbon budget 1959–2011, Earth Syst. Sci. Data, 5, 165–185, doi:10.5194/essd-5-165-2013, 2013.

Levy, P. E., Cannell, M. G. R., and Friend, A. D.: Modelling the impact of future changes in climate, $CO_2$ concentration and land use on natural ecosystems and the terrestrial carbon sink, Global Environ. Chang., 14, 21–30, 2004.

Lewis, S. L., Lopez-Gonzalez, G., Sonké, B., Affum-Baffoe, K., Baker, T. R., Ojo, L. O., Phillips, O. L., Reitsma, J. M., White, L., James, A., Comiskey, K., Djuikouo, M.-N., Ewango, C. E. N., Feldpausch, T. R., Hamilton, A. C., Gloor, M., Hart, T., Hladik, A., Lloyd, J., Lovett, J. C., Makana, J.-R., Malhi, Y., Mbago, F. M., Ndangalasi, H. J., Peacock, J., Peh, K. S.-H., Sheil, D., Sunderland, T., Swaine, M. D., Taplin, J., Taylor, D., Thomas, S. C., and Wöll, R. V. H.: Increasing carbon storage in intact African tropical forests, Nature, 457, 1003–1006, 2009a.

Lewis, S. L., Lloyd, J., Sitch, S., Mitchard, E. T. A., and Laurance, W. F.: Changing Ecology of Tropical Forests: Evidence and Drivers, Annu. Rev. Ecol. Evol. Syst., 40, 529–49, 2009b.

Lovenduski, N. S., Gruber, N., Doney, S. C., and Lima, I. D.: Enhanced $CO_2$ outgassing in the Southern Ocean from a positive phase of the Southern Annular Mode, Global Biogeochem. Cy. 21, GB2026, doi:10.1029/2006GB002900, 2007.

Lovenduski, N. S., Gruber, N., and Doney, S. C.: Toward a mechanistic understanding of the decadal trends in the Southern Ocean carbon sink, Global Biogeochem. Cy., 22, 1–9, 2008.

Lucht, W., Prentice, I. C., Myneni, R. B., Sitch, S., Friedlingstein, P., Cramer, W., Bousquet, P., Buermann, W., and Smith, B.: Climate control of the high-latitude vegetation greening trend and Pinatubo effect, Science, 296, 1687–1689, 2002.

Luo, Y. Q., Randerson, J. T., Abramowitz, G., Bacour, C., Blyth, E., Carvalhais, N., Ciais, P., Dalmonech, D., Fisher, J. B., Fisher, R., Friedlingstein, P., Hibbard, K., Hoffman, F., Huntzinger, D., Jones, C. D., Koven, C., Lawrence, D., Li, D. J., Mahecha, M., Niu, S. L., Norby, R., Piao, S. L., Qi, X., Peylin, P., Prentice, I. C., Riley, W., Reichstein, M., Schwalm, C., Wang, Y. P., Xia, J. Y., Zaehle, S., and Zhou, X. H.: A framework for benchmarking land models, Biogeosciences, 9, 3857–3874, doi:10.5194/bg-9-3857-2012, 2012.

Luyssaert, S., Abril, G., Andres, R., Bastviken, D., Bellassen, V., Bergamaschi, P., Bousquet, P., Chevallier, F., Ciais, P., Corazza, M., Dechow, R., Erb, K.-H., Etiope, G., Fortems-Cheiney, A., Grassi, G., Hartmann, J., Jung, M., Lathière, J., Lohila, A., Mayorga, E., Moosdorf, N., Njakou, D. S., Otto, J., Papale, D., Peters, W., Peylin, P., Raymond, P., Rödenbeck, C., Saarnio, S., Schulze, E.-D., Szopa, S., Thompson, R., Verkerk, P. J., Vuichard, N., Wang, R., Wattenbach, M., and Zaehle, S.: The European land and inland water $CO_2$, CO, $CH_4$ and $N_2O$ balance between 2001 and 2005, Biogeosciences, 9, 3357–3380, doi:10.5194/bg-9-3357-2012, 2012.

Manning, A. C. and Keeling, R. F.: Global oceanic and land biota sinks from the Scripps atmospheric oxygen flask sampling network, Tellus B, 58B, 95–116, 2006.

Matear, R. J., Chamberlain, M. A., Sun, C. and Feng, M.: Climate change projection of the Tasman Sea from an Eddy-resolving Ocean Model, J. Geophys. Res.-Oceans, 118, 2961–2976, doi:10.1002/jgrc.20202, 2013.

Matsumoto, K. and Gruber, N.: How accurate is the estimation of anthropogenic carbon in the ocean?, An evaluation of the DC* method, Global Biogeochem. Cy., 19, GB3014, doi:10.1029/2004GB002397, 2005.

McDonald, K. C., Kimball, J. S., Njoke, E., Zimmermann, R., and Zhao, M.: Variability in springtime thaw in the terrestrial high latitudes: monitoring a major control on the biospheric assimilation of atmospheric $CO_2$ with spaceborne microwave remote sensing, Earth Interact., 8, 1–23, 2004.

McDowell, N. G, Pockman, W. T., Allen, C. D., Breshears, D. D., Cobb, N., Kolb, T., Plaut, J., Sperry, J., West, A., Williams, D. G., and Yepez, E. A.: Mechanisms of plant survival and mortality during drought: why do some plants survive while others succumb to drought?. New Phytol., 178, 719–739, 2008.

McGillicuddy Jr, D. J., Robinson, A. R., Siegel, D. A., Jannasch, H. W., Johnson, R., Dickey, T. D., McNeil, J., Michaels, A. F., and Knap, A. H.: Influence of mesoscale eddies on new production in the Sargasso Sea, Nature, 394, 263–266, 1998.

McGuire, A. D., Christensen, T. R., Hayes, D., Heroult, A., Euskirchen, E., Kimball, J. S., Koven, C., Lafleur, P., Miller, P. A., Oechel, W., Peylin, P., Williams, M., and Yi, Y.: An assessment of the carbon balance of Arctic tundra: comparisons among observations, process models, and atmospheric inversions, Biogeosciences, 9, 3185–3204, doi:10.5194/bg-9-3185-2012, 2012.

McKinley, G. A., Takahashi, T., Buitenhuis, E., Chai, F., Christian, J. R., Doney, S. C., Jiang, M.-S., Le Quéré, C., Lima, I., Linday, K., Moore, J. K., Murtugudde, R., Shi, L., and Wetzel, P.: North Pacific carbon cycle response to climate variability on seasonal to decadal timescales. J. Geophys. Res., 111, C07S06, doi:10.1029/2005JC003173, 2006.

McKinley, G. A., Fay, A. R., Takahashi, T., and Metzl, N: Convergence of atmospheric and North Atlantic carbon dioxide trends on multidecadal timescales, Nat. Geosci, 4, 606–610, doi:10.1038/NGEO1193, 2011.

McNeil, B. I. and Matear, R. J.: The non-steady state oceanic $CO_2$ signal: its importance, magnitude and a novel way to detect it, Biogeosciences, 10, 2219–2228, doi:10.5194/bg-10-2219-2013, 2013.

Mercado, L. M., Bellouin, N., Sitch, S., Boucher, O., Huntingford, C., and Cox, P. M.: Impact of Changes in Diffuse Radiation on the Global Land Carbon Sink, Nature, 458, 1014–1017, 2009.

Mikaloff Fletcher, S. E., Gruber, N., Jacobson, A. R., Doney, S. C., Dutkiewicz, S., Gerber, M., Follows, M., Joos, F., Lindsay, K., Menemenlis, D., Mouchet, A., Müller, S. A., and Sarmiento, J. L.: Inverse estimates of anthropogenic $CO_2$ uptake, transport, and storage by the oceans, Global Biogeochem. Cy., 20, GB2002, doi:10.1029/2005GB002530, 2006.

Morales, P., Sykes, M. T., Prentice, I. C., Smith, P., Smith, B., Bugmann, H., Zierl, B., Friedlingstein, P., Viovy, N., Sabaté, S., Sánchez, A., Pla, E., Gracia, C. A., Sitch, S., Arneth, A., and Ogee, J.: Comparing and evaluating process-based ecosystem model predictions of carbon and water fluxes in major European forest biomes, Glob. Change Biol., 11, 2211–2233, doi:10.1111/j.1365-2486.2005.01036.x, 2005.

Myneni, R. B., Keeling, C. D., Tucker, C. J., Asrar, G., and Nemani, R. R.: Increased plant growth in the northern high latitudes from 1981 to 1991, Nature, 386, 698–702, doi:10.1038/386698a0, 1997.

Murray-Tortarolo, G., Anav, A., Friedlingstein, P., Sitch, S., Piao, S., Zhu, Z., Poulter, B., Zaehle, S., Ahlstrom, A., Lomas, M., Levis, S., Viovy, N., and Zeng, N.: Evaluation of DGVMs in reproducing satellite derived LAI over the Northern Hemisphere, Part I: Uncoupled DGVMs, Remote Sens., 5, 4819–4838; doi:10.3390/rs5104819, 2013.

Müller, S. A., Joos, F., Plattner, G.-K., Edwards, N. R., and Stocker, T. F.: Modeled natural and excess radiocarbon: Sensitivities to the gas exchange formulation and ocean transport strength, Global Biogeochem. Cy., 22, doi:10.1029/2007GB003065, 2008.

Nemani, R. R., Keeling, C. D., Hashimoto, H., Jolly, W. M., Piper, S. C., Tucker, C. J., Myneni, R. B., and Running, S. W.: Climate-driven increases in global terrestrial net primary production from 1982 to 1999, Science, 300, 1560–1563, 2003.

New, M. G., Hulme, M., and Jones, P. D.: Representing twentieth-century space-climate variability, Part II, Development of 1901–1996 monthly grids of terrestrial surface climate, J. Climate, 13, 2217–2238, 2000.

Norby, R. J., DeLucia, E. H., Gielen, B., Calfapietra, C., Giardina, C. P., King, J. S., Ledford, J., McCarthy, H. R., Moore, D. J. P., Ceulemans, R., De Angelis, P., Finzi, A. C., Karnosky, D. F., Kubiske, M. E., Lukac, M., Pregitzer, K. S., Scarascia-Mugnozza, G. E., Schlesinger, W. H., and Oren, R.: Forest response to elevated CO2 is conserved across a broad range of productivity, P. Natl. Acad. Sci. USA, 102, 18052–18056, 2005.

Norby, R. J., Warren, J. M., Iversen, C. M., Medlyn, B. E., and McMurtrie, R. E.: $CO_2$ enhancement of forest productivity constrained by limited nitrogen availability, P. Natl. Acad. Sci., 107, 19368–19373, 2010.

Oleson, K. W., Lawrence, D. M., Bonan, G. B., Flanner, M. G., Kluzek, E., Lawrence, P. J., Levis, S., Swenson, S. C., and Thornton, P. E.: Technical description of version 4.0 of the Community Land Model (CLM), NCAR Tech. Note NCAR/TN-478+STR, 257 pp., 2010.

Pacala, S. W., Hurtt, G. C., Baker, D., Peylin, P., Houghton, R. A., Birdsey, R. A., Heath, L., Sundquist, E. T., Stallard, R. F., Ciais, P., Moorcroft, P., Caspersen, J. P., Shevliakova, E., Moore B., Kohlmaier, G., Holland, E., Gloor, M., Harmon, M. E., Fan, S.-M., Sarmiento, J. L., Goodale, C. L., Schimel, D., and Field, C. B.: Consistent land- and atmosphere-based US carbon sink estimates, Science, 292, 2316–2320, 2001.

Pan, Y., Birdsey, R.A., Fang, J., Houghton, R., Kauppi, P. E., Kurz, W. A., Phillips, O. L., Shvidenko, A., Lewis, S. L., Canadell, J. G., Ciais, P., Jackson, R. B., Pacala, S., McGuire, A. D., Piao, S., Rautiainen, A., Sitch, S., Hayes, D., and Watson, C.: A large and persistent carbon sink in the World's forests, 1990–2007, Science, doi:10.1126/science.1201609, 2011.

Park, G.-H., Wanninkhof, R., Doney, S. C., Takahashi, T., Lee, K., Feely, R. A., Sabine, C. L., Triñanes, J., and Lima, I. D.: Variability of global net sea-air $CO_2$ fluxes over the last three decades using empirical relationships, Tellus B, 62, 352–368, 2010.

Patra, P. K., Canadell, J. G., Houghton, R. A., Piao, S. L., Oh, N.-H., Ciais, P., Manjunath, K. R., Chhabra, A., Wang, T., Bhattacharya, T., Bousquet, P., Hartman, J., Ito, A., Mayorga, E., Niwa, Y., Raymond, P. A., Sarma, V. V. S. S., and Lasco, R.: The carbon budget of South Asia, Biogeosciences, 10, 513–527, doi:10.5194/bg-10-513-2013, 2013.

Peacock, S.: Debate over the ocean bomb radiocarbon sink: Closing the gap, Global Biogeochem. Cy., 18, GB2022, doi:10.1029/2003GB002211, 2004.

Peng S., Ciais, P., Chevallier, F., Peylin, P., Cadule, P., Sitch, S., Piao, S., Ahlström, A., Levy, P., Lomas, M., Poulter, B., Viovy, N., Wang, T., Zaehle, S., Zeng, N., Zhao, F. and Zhao, H.: Benchmarking the seasonal cycle of $CO_2$ fluxes simulated by terrestrial ecosystem models, Global Biogeochem. Cy., 29, doi:10.1002/2014GB004931, 2014.

Peylin, P., Bousquet, P., Le Quéré, C., Sitch, S., Friedlingstein, P., McKinley, G., Gruber, N., Rayner, P., and Ciais, P.: Multiple constraints on regional $CO_2$ flux variations over land and oceans, Global Biogeochem. Cy., 19, GB1011, doi:10.1029/2003GB002214, 2005.

Peylin, P., Law, R. M., Gurney, K. R., Chevallier, F., Jacobson, A. R., Maki, T., Niwa, Y., Patra, P. K., Peters, W., Rayner, P. J., Rödenbeck, C., van der Laan-Luijkx, I. T., and Zhang, X.: Global atmospheric carbon budget: results from an ensemble of atmospheric $CO_2$ inversions, Biogeosciences, 10, 6699–6720, doi:10.5194/bg-10-6699-2013, 2013.

Pfeil, B., Olsen, A., Bakker, D. C. E., Hankin, S., Koyuk, H., Kozyr, A., Malczyk, J., Manke, A., Metzl, N., Sabine, C. L., Akl, J., Alin, S. R., Bates, N., Bellerby, R. G. J., Borges, A., Boutin, J., Brown, P. J., Cai, W.-J., Chavez, F. P., Chen, A., Cosca, C., Fassbender, A. J., Feely, R. A., González-Dávila, M., Goyet, C., Hales, B., Hardman-Mountford, N., Heinze, C., Hood, M., Hoppema, M., Hunt, C. W., Hydes, D., Ishii, M., Johannessen, T., Jones, S. D., Key, R. M., Körtzinger, A., Landschützer, P., Lauvset, S. K., Lefèvre, N., Lenton, A., Lourantou, A., Merlivat, L., Midorikawa, T., Mintrop, L., Miyazaki, C., Murata, A., Nakadate, A., Nakano, Y., Nakaoka, S., Nojiri, Y., Omar, A. M., Padin, X. A., Park, G.-H., Paterson, K., Perez, F. F., Pierrot, D., Poisson, A., Ríos, A. F., Santana-Casiano, J. M., Salisbury, J., Sarma, V. V. S. S., Schlitzer, R., Schneider, B., Schuster, U., Sieger, R., Skjelvan, I., Steinhoff, T., Suzuki, T., Takahashi, T., Tedesco, K., Telszewski, M., Thomas, H., Tilbrook, B., Tjiputra, J., Vandemark, D., Veness, T., Wanninkhof, R., Watson, A. J., Weiss, R., Wong, C. S., and Yoshikawa-Inoue, H.: A uniform, quality controlled Surface Ocean $CO_2$ Atlas (SOCAT), Earth Syst. Sci. Data, 5, 125–143, doi:10.5194/essd-5-125-2013, 2013.

Phillips, O. L., Malhi, Y., Higuchi, N., Laurance, W. F., Nunez, P. V., Vasquez, R. M., Laurance, S. G., Ferreira, L. V., Stern, M., Brown, S., and Grace, J.: Changes in the carbon balance of tropical forests: Evidence from long-term plots, Science, 282, 439–442, 1998.

Piao, S. L., Fang, J. Y., Ciais, P., Peylin, P., Huang, Y., Sitch, S., and Wang, T: The carbon balance of terrestrial ecosystems in China, Nature, 458, 1009–1014, 2009.

Piao, S. L., Sitch, S., Ciais, P., Friedlingstein, P., Peylin, P., Wang, X. H., Ahlström, A., Anav, A., Canadell, J. G., Huntingford, C., Jung, M., Levis, S., Levy, P. E., Li, J. S., Lin, X., Lomas, M. R., Lu, M ., Luo, Y. Q., Ma, Y. C., Myneni, R. B., Poulter, B., Sun, Z. Z., Wang, T., Viovy, N., Zaehle, S., and Zeng, N.: Evaluation of terrestrial carbon cycle models for their response to climate variability and to $CO_2$ trends, Glob. Change Biol., 19, 2117–2132, 2013.

Pongratz, J., Reick, C. H., Houghton, R. A., and House, J. I.: Terminology as a key uncertainty in net land use and land cover change carbon flux estimates, Earth Syst. Dynam., 5, 177–195, doi:10.5194/esd-5-177-2014, 2014.

Poulter, B., Frank, D. C., Hodson, E. L., and Zimmermann, N. E.: Impacts of land cover and climate data selection on understanding terrestrial carbon dynamics and the $CO_2$ airborne fraction, Biogeosciences, 8, 2027–2036, doi:10.5194/bg-8-2027-2011, 2011.

Poulter, B., Pederson, N., Liu, H., Zhu, Z., D'Arrigo, R., Ciais, P., Davi, N., Frank, D., Leland, C., Myneni, R., Piao, S., and Wang, T.: Recent trends in Inner Asian forest dynamics to temperature and precipitation indicate high sensitivity to climate change, Agr. Forest Meteorol., 178–179, 31–45, 2013.

Poulter, B., Frank, D., Ciais, P., Myneni, R., Andela, N., Bi, J., Broquet, G., Canadell, J. G., Chevallier, F., Liu, Y. Y., Running, S. W., Sitch, S. and van der Werf, G. R.: Contribution of semi-arid ecosystems to interannual variability of the global carbon cycle, Nature, doi:10.1038/nature13376, 2014.

Prentice I. C., Farquhar, G. D., Fasham, M. J. R., Goulden, M. L., Heimann, M., Jaramillo, V.J., Kheshgi, H. S., Le Quere, C., Scholes, R. J., Wallace, D. W. R., Contributing Authors Archer, D., Ashmore, M. R., Aumont, O., Baker, D., Battle, M., Bender,

M., Bopp, L. P., Bousquet, P., Caldeira, K., Ciais, P., Cox, P. M., Cramer, W., Dentener, F., Enting, I. G., Field, C. B., Friedlingstein, P., Holland, E. A., Houghton, R. A., House, J. I., Ishida, A., Jain, A. K., Janssens, I. A., Joos, F., Kaminski, T., Keeling, C. D., Keeling, R. F., Kicklighter, D. W., Kohfeld, K. E., Knorr, W., Law, R., Lenton, T. , Lindsay, K., Maier-Reimer, E., Manning, A. C., Matear, R. J., McGuire, A. D., Melillo, J. M., Meyer, R., Mund, M., Orr, J. C., Piper, S., Plattner, K., Rayner, P. J., Sitch, S., Slater, R., Taguchi, S. , Tans, P. P., Tian, H. Q., Weirig, M. F., Whorf, T., and Yool, A.: The carbon cycle and atmospheric carbon dioxide, in. Climate Change 2001: The Scientific Basis edited by: Houghton, J. T., Cambridge Univ. Press, New York, 183–237, 2001.

Prentice, I. C., Bondeau, A., Cramer, W., Harrison, S. P., Hickler, T., Lucht, W., Sitch, S., Smith, B., and Sykes, M. T.: Terrestrial Ecosystems in a changing world, IGBP Book Series, edited by: Canadell. J., Pitelka, L., and Pataki, D., Springer, Heidelberg, Germany, pp. 336, 2007.

Quaife, T., Quegan, S., Disney, M., Lewis, P., Lomas, M. R., and Woodward, F. I.: Impact of land cover uncertainties on estimates of biospheric carbon fluxes, Global Biogeochem. Cy., 22, GB4016, doi:10.1029/2007GB003097, 2008.

Randerson, J. T., Hoffman, F. M., Thornton, P. E., Mahowald, N. M., Lindsay, K., Lee, Y.-H., Nevison, C. D., Doney, S. C., Bonan, G., Stoeckli, R., Covey, C., Running, S. W., and Fung, I. Y.: Systematic assessment of terrestrial biogeochemistry in coupled climate-carbon models, Glob. Change Biol., 15, 2462–2484, 2009.

Raupach, M. R., Canadell, J. G., and Le Quéré, C.: Anthropogenic and biophysical contributions to increasing atmospheric CO2 growth rate and airborne fraction, Biogeosciences, 5, 1601–1613, doi:10.5194/bg-5-1601-2008, 2008.

Raupach, M. R., Gloor, M., Sarmiento, J. L., Canadell, J. G., Frölicher, T. L., Gasser, T., Houghton, R. A., Le Quéré, C., and Trudinger, C. M.: The declining uptake rate of atmospheric $CO_2$ by land and ocean sinks, Biogeosciences, 11, 3453–3475, doi:10.5194/bg-11-3453-2014, 2014.

Reichstein, M., Bahn, M., Ciais, P., Frank, D., Mahecha, M. D., Seneviratne, S. I., Zscheischler, J., Beer, C., Buchmann, N., Frank, D. C., Papale, D., Rammig, A., Smith, P., Thonicke, K., van der Velde, M., Vicca, S., Walz, A., and Wattenbach, M.: Climate extremes and the carbon cycle, Nature, 500, 287–295, 2013.

Roy, T., Bopp, L., Gehlen, M., Schneider, B., Cadule, P., Frölicher, T. L., Segschneider, J., Tjiputra, J., Heinze, C., and Joos, F.: Regional Impacts of Climate Change and Atmospheric $CO_2$ on Future Ocean Carbon Uptake: A Multimodel Linear Feedback Analysis, J. Climate, 24, 2300–2318, 2011.

Sabine, C. S., Feely, R. A.., Gruber, N. , Key, R. M., Lee, K., Bullister, J. L., Wanninkhof, R., Wong, C. S., Wallace, D. W. R., Tillbrook, B., Millero, F. J., Peng, T.-H., Kozyr, A., Ono, T., and Rios, A. F.: The oceanic sink for anthropogenic $CO_2$, Science, 305, 367–371, 2004.

Sarmiento, J. L. and Gruber, N.: Sinks for anthropogenic carbon, Phys. Today, 55, 30–36, 2002.

Sarmiento, J. L. and Gruber, N.: Ocean Biogeochemical Dynamics, Princeton Univ. Press, 526 pp., 2006.

Sarmiento, J. L., Orr, J. C., and Siegenthaler, U.: A perturbation simulation of $CO_2$ uptake in an ocean general circulation model, J. Geophys. Res., 97, 3621–3645, 1992.

Sarmiento, J. L., Gloor, M., Gruber, N., Beaulieu, C., Jacobson, A. R., Mikaloff Fletcher, S. E., Pacala, S., and Rodgers, K.: Trends and regional distributions of land and ocean carbon sinks, Biogeosciences, 7, 2351–2367, doi:10.5194/bg-7-2351-2010, 2010.

Schuster, U., McKinley, G. A., Bates, N., Chevallier, F., Doney, S. C., Fay, A. R., González-Dávila, M., Gruber, N., Jones, S., Krijnen, J., Landschützer, P., Lefèvre, N., Manizza, M., Mathis, J., Metzl, N., Olsen, A., Rios, A. F., Rödenbeck, C., Santana-Casiano, J. M., Takahashi, T., Wanninkhof, R., and Watson, A. J.: An assessment of the Atlantic and Arctic sea-air $CO_2$ fluxes, 1990–2009, Biogeosciences, 10, 607–627, doi:10.5194/bg-10-607-2013, 2013.

Sitch, S., Smith, B., Prentice, I. C., Arneth, A., Bondeau, A., Cramer, W., Kaplan, J. O., Levis, S., Lucht, W., Sykes, M. T., Thonicke, K., and Venevsky, S.: Evaluation of ecosystem dynamics, plant geography and terrestrial carbon cycling in the LPJ dynamic global vegetation model, Glob. Change Biol., 9, 161–185, doi:10.1046/j.1365-2486.2003.00569.x, 2003.

Sitch, S., McGuire, A. D., Kimball, J., Gedney, N., Gamon, J., Engstrom, R., Wolf, A., Zhuang, Q., Clein, J. S., and McDonald, K. C.: Assessing the carbon balance of circumpolar arctic tundra using remote sensing and process modeling, Ecol. Appl., 17, 213–234, 2007a.

Sitch, S., Cox, P. M., Collins, W. J., and Huntingford., C.: Indirect radiative forcing of climate change through ozone effects on the land-carbon sink, Nature, 448, 791–794, doi:10.1038/nature06059, 2007b.

Sitch, S., Huntingford, C., Gedney, N., Levy, P. E., Lomas, M., Piao, S., Betts, R., Ciais, P., Cox, P., Friedlingstein, P., Jones, C. D., Prentice, I. C., and Woodward, F. I.: Evaluation of the terrestrial carbon cycle, future plant geography, and climate-carbon cycle feedbacks using 5 Dynamic Global Vegetation Models (DGVMs), Glob. Change Biol., 14 1–25, doi:10.1111/j.1365-2486.2008.01626.x, 2008.

Smith, B., Prentice, I. C., and Sykes, M. T.: Representation of vegetation dynamics in the modelling of terrestrial ecosystems: comparing two contrasting approaches within European climate space, Global Ecol. Biogeogr., 10, 621–637, 2001.

Sokolov, A. P., Kicklighter, D. W., Melillo, J. M., Felzer, B. S., Schlosser, C. A., and Cronin, T. W.: Consequences of considering carbon-nitrogen interactions on the feedbacks between climate and the terrestrial carbon cycle, J. Climate, 21, 3776–3796, doi:10.1175/2008JCLI2038.1, 2008.

Stocker, B. D., Feissli, F., Strassmann, K. M., Spahni, R., and Joos, F.: Past and future carbon fluxes from land use change, shifting cultivation and wood harvest, Tellus B, 66, 23188, doi:10.3402/tellusb.v66.23188, 2014.

Stephens, B. B., Gurney, K. R., Tans, P. P., Sweeney, C., Peters, W., Bruhwiler, L., Ciais, P., Ramonet, M., Bousquet, P., Nakazawa, T., Aoki, S., Machida, T., Inoue, G., Vinnichenko, N., Lloyd, J., Jordan, A., Heimann, M., Shibistova, O., Langenfelds, R. L., Steele, L. P., Francey, R. J., and Denning, A. S.: Weak northern and strong tropical land carbon uptake from vertical profiles of atmospheric $CO_2$, Science, 316, 1732–1735, 2007.

Sweeney, C., Gloor, E., Jacobson, A. R., Key, R. M., McKinley, G., Sarmiento, J. L., and Wanninkhof, R.: Constraining global air-sea gas exchange for $CO_2$ with recent bomb $^{14}C$ measurements, Global Biogeochem. Cycl., 21, GB2015, doi:10.1029/2006GB002784, 2007.

Takahashi, T., Sutherland, S. C., Wanninkhof, R., Sweeney, C., Feely, R. A., Chipman, D., Hales, B., Friederich, G., Chavez, F., Sabine, C., Watson, A., Bakker, D. C. E., Schuster, U., Metzl, N., Yoshikawa-Inoue, H., Ishii, M., Midorikawa, T., Nojiri, Y., Kortzinger, A., Steinhoff, T., Hoppema, M., Olafsson, J., Arnarson, T. S., Tilbrook, B., Johannessen, T., Olsen, A., Bellerby, R., Wong, C. S., Delille, B., Bates, N. R., and de Baar, H. J. W.: Climatological mean and decadal changes in surface ocean $pCO_2$, and net sea-air CO2 flux over the global oceans, SOCOVV Symposium Volume, Deep Sea Res.-Pt. II, 810, 554–577, 2009.

Tans, P. P., Fung, I. Y., and Takahashi, T.: Observational constraints on the global atmospheric $CO_2$ budget, Science, 247, 1431–1439, doi:10.1126/science.247.4949.1431, 1990.

Thornton, P. E., Lamarque, J. F., Rosenbloom, N. A., and Mahowald, N. M.: Influence of carbon-nitrogen cycle coupling on land model response to $CO_2$ fertilization and climate variability, Global Biogeochem. Cy., 21, GB4018, doi:10.1029/2006GB002868, 2007.

Thornton, P. E., Doney, S. C., Lindsay, K., Moore, J. K., Mahowald, N., Randerson, J. T., Fung, I., Lamarque, J.-F., Feddema, J. J., and Lee, Y.-H.: Carbon-nitrogen interactions regulate climate-carbon cycle feedbacks: results from an atmosphere-ocean general circulation model, Biogeosciences, 6, 2099–2120, doi:10.5194/bg-6-2099-2009, 2009.

Tjiputra, J. F., Assmann, K., and Heinze, C.: Anthropogenic carbon dynamics in the changing ocean, Ocean Science, 6, 605–614, 2010.

Tucker, C. J., Slayback, D. A., Pinzon, J. E., Los, S. O., Myneni, R. B., and Taylor, M. G.: Higher northern latitude normalized difference vegetation index and growing season trends from 1982 to 1999, Int. J. Biometeorol., 45, 184–190, 2001.

Valentini, R., Arneth, A., Bombelli, A., Castaldi, S., Cazzolla Gatti, R., Chevallier, F., Ciais, P., Grieco, E., Hartmann, J., Henry, M., Houghton, R. A., Jung, M., Kutsch, W. L., Malhi, Y., Mayorga, E., Merbold, L., Murray-Tortarolo, G., Papale, D., Peylin, P., Poulter, B., Raymond, P. A., Santini, M., Sitch, S., Vaglio Laurin, G., van der Werf, G. R., Williams, C. A., and Scholes, R. J.: A full greenhouse gases budget of Africa: synthesis, uncertainties, and vulnerabilities, Biogeosciences, 11, 381–407, doi:10.5194/bg-11-381-2014, 2014.

Van der Molen, M. K., Dolman, A. J., Ciais, P., Eglin, T., Gobron, N., Law, B. E., Meir, P., Peters, W., Phillips, O. L., Reichstein, M., Chen, T., Dekker, S. C., Doubková, M., Friedl, M. A., Jung, M., van den Hurk, B. J. J. M., de Jeu, R. A. M., Kruijt, B., Ohta, T., Rebel, K. T., Plummer, S., Seneviratne, S. I., Sitch, S., Teuling, A. J., van der Werf, G. R., and Wang, G.: Drought and ecosystem carbon cycling, Agr. Forest Meteorol., 151, 765–773, doi:10.1016/j.agrformet.2011.01.018, 2011.

Vitousek, P. M. and Howarth, R. W.: Nitrogen limitation on land and in the sea: How can it occur?, Biogeochemistry, 13, 87–115, 1991.

Wang, Y. P., Law, R. M., and Pak, B.: A global model of carbon, nitrogen and phosphorus cycles for the terrestrial biosphere, Biogeosciences, 7, 2261–2282, doi:10.5194/bg-7-2261-2010, 2010.

Wanninkhof, R.: Relationship between wind speed and gas exchange over the ocean, J. Geophys. Res., 97, 7373–7382, 1992.

Wanninkhof, R., Park, G. -H., Takahashi, T., Sweeney, C., Feely, R., Nojiri, Y., Gruber, N., Doney, S. C., McKinley, G. A., Lenton, A., Le Quéré, C., Heinze, C., Schwinger, J., Graven, H., and Khatiwala, S.: Global ocean carbon uptake: magnitude, variability and trends, Biogeosciences, 10, 1983–2000, doi:10.5194/bg-10-1983-2013, 2013.

Woodward, F. I. and Lomas, M. R.: Vegetation-dynamics-simulating responses to climate change, Biological Reviews, 79, 643–670, 2004.

Woodward, F. I., Smith, T. M., Emanuel, W. R.: A global land primary productivity and phytogeography model. Global Biogeochem. Cy., 9, 471–490, 1995.

Zaehle, S. and Friend, A. D.: Carbon and nitrogen cycle dynamics in the O-CN land surface model, I: Model description, site- scale evaluation and sensitivity to parameter estimates, Global Biogeochem. Cy., 24, GB1005, doi:10.1029/2009GB003521, 2010.

Zaehle, S. and Dalmonech, D.: Carbon – nitrogen interactions on land at global scales: current understanding in modeling climate biosphere feedbacks, Current Opinion in Environmental Sustainability, 3, 311–320, 2011.

Zaehle, S., Friedlingstein, P., and Friend, A. D.: Terrestrial nitrogen feedbacks may acccelerate future climate change, Geophys. Res. Lett., 37, L01401, doi:10.1029/2009GL041345, 2010.

Zaehle, S., Ciais, P., Friend, A. D., and Prieur, V.: Carbon benefits of anthropogenic reactive nitrogen offset by nitrous oxide emissions, Nat. Geosci., 4, 601–605, doi:10.1038/ngeo1207, 2011.

Zaehle, S., Medlyn, B. E., De Kauwe, M. G., Walker, A. P., Dietze, M. C., Hickler, T., Luo, Y., Wany, Y.-P., El-Masri, B., Thornton, P., Jain, A., Wang, S., Warlind, D., Weng, E., Parton, W., Iversen, C. M., Gallet-Budynek, A., McCarthy, H., Finzi, A., Hanson, P. J., Prentice, I. C., Oren, R., and Norby, R. J.: Evaluation of eleven terrestrial carbon-nitrogen cycle models against observations from two temperate Free-Air $CO_2$ Enrichment Studies, New Phytologist, 202, 803–822, doi:10.1111/nph.12697, 2014.

Zeng, N.: Glacial-interglacial atmospheric $CO_2$ change – The glacial burial hypothesis, Adv. Atmos. Sci., 20, 677–673, 2003.

Zeng, N., Mariotti, A., and Wetzel, P.: Terrestrial mechanisms of interannual $CO_2$ variability, Global Biogeochem. Cy., 19, GB1016, doi:10.1029/2004gb002273, 2005.

Zhang, Q., Wang, Y. P., Matear, R. J., Pitman, A. J., and Dai, Y. J.: Nitrogen and phosphorous limitations significantly reduce future allowable $CO_2$ emissions, Geophys. Res. Lett, 41, 632–637, doi:10.1002/2013GL058352, 2014.

Zhu, Z., Bi, J., Pan, Y., Ganguly, S., Anav, A., Xu, L., Samanta, A., Piao, S., Nemani, R. R., and Myneni, R. B.: Global Data Sets of Vegetation Leaf Area Index (LAI)3g and Fraction of Photosynthetically Active Radiation (FPAR)3g Derived from Global Inventory Modeling and Mapping Studies (GIMMS) Normalized Difference Vegetation Index (NDVI3g) for the Period 1981 to 2011, Remote Sens., 5, 927–948, 2013.

Zscheischler, J., Mahecha, M. D., von Buttlar, J., Harmeling, S., Jung, M., Rammig, A., Randerson, J. T., Schoelkopf, B., Seneviratne, S. I., Tomelleri, E., Zaehle, S., and Reichstein, M.: A few extreme events dominate global interannual variability in gross primary production, Environ. Res. Lett., 9, 035001, doi:10.1088/1748-9326/9/3/035001, 2014.